INFLUENCE OF INSTRUMENT TRANSFORMERS ON POWER SYSTEM PROTECTION

A Thesis

by

BOGDAN NAODOVIC

Submitted to the Office of Graduate Studies of
Texas A&M University
in partial fulfillment of the requirements for the degree of

MASTER OF SCIENCE

May 2005

Major Subject: Electrical Engineering

INFLUENCE OF INSTRUMENT TRANSFORMERS ON

POWER SYSTEM PROTECTION

A Thesis

by

BOGDAN NAODOVIC

Submitted to Texas A&M University
in partial fulfillment of the requirements
for the degree of

MASTER OF SCIENCE

Approved as to style and content by:

Mladen Kezunovic
(Chair of Committee)

Ali Abur
(Member)

Krishna R. Narayanan
(Member)

William M. Lively
(Member)

Chanan Singh
(Head of Department)

May 2005

Major Subject: Electrical Engineering

ABSTRACT

Influence of Instrument Transformers on
Power System Protection. (May 2005)

Bogdan Naodovic, B.S., University of Novi Sad, Serbia and Montenegro
Chair of Advisory Committee: Dr. Mladen Kezunovic

Instrument transformers are a crucial component of power system protection. They supply the protection system with scaled-down replicas of current and voltage signals present in a power network to the levels which are safe and practical to operate with. The conventional instrument transformers are based on electromagnetic coupling between the power network on the primary side and protective devices on the secondary. Due to such a design, instrument transformers insert distortions in the mentioned signal replicas. Protective devices may be sensitive to these distortions. The influence of distortions may lead to disastrous misoperations of protective devices. To overcome this problem, a new instrument transformer design has been devised: optical sensing of currents and voltages. In the theory, novel instrument transformers promise a distortion-free replication of the primary signals. Since the mentioned novel design has not been widely used in practice so far, its superior performance needs to be evaluated. This poses a question: how can the new technology (design) be evaluated, and compared to the existing instrument transformer technology? The importance of this question lies in its consequence: is there a necessity to upgrade the protection system, i.e. to replace the conventional instrument transformers with the novel ones, which would be quite expensive and time-consuming?

The posed question can be answered by comparing influences of both the novel and the conventional instrument transformers on the protection system. At present, there is no systematic approach to this evaluation. Since the evaluation could lead to an improvement of the overall protection system, this thesis proposes a comprehensive and systematic methodology for the evaluation. The thesis also proposes a complete solution for the evaluation, in the form of a simulation environment. Finally, the thesis presents results of evaluation, along with their interpretation.

ACKNOWLEDGMENTS

I would like to express sincere gratitude to my family and my friends, whose support helped me immensely during my research. Sincere thanks and gratitude are also given to my teachers and committee members.

TABLE OF CONTENTS

CHAPTER Page

LIST OF TABLES

TABLE Page

TABLE Page

LIST OF FIGURES

FIGURE Page

FIGURE Page

CHAPTER I

INTRODUCTION

A. Background

Objective of every power system is maintaining uninterrupted operation [1]. Protection is a part of power system, which ensures that effects of eventual faulty conditions are minimized. One of the crucial components of protection system are instrument transformers [2]. They provide access to high-magnitude currents and voltages on the power network, by supplying protection with signal replicas scaled-down to levels that are safe and practical (for use by protective gear). Correct and timely identification of faults and disturbances (in the network) is dependent on accuracy of mentioned signal replicas. Consequently, protection system operation is dependant on performance of instrument transformers.

B. Definition of the Problem

The vast majority of instrument transformers installed today are conventional. Conventional instrument transformers are based on electromagnetic coupling between power network on the primary side, and protective devices on the secondary side [3]. Inherent to this coupling are *signal distortions* in various forms. These distortions are, in a sense, artificial: they do not originate from the power network, but are inserted by the coupling within the instrument transformers.

Protective devices may be sensitive to signal distortions, regardless of their source. Field application has shown that this sensitivity may lead to disastrous miss-

---

This thesis follows the style of *IEEE Transactions on Power Delivery.*

operations. To overcome this problem, two main approaches can be identified:

1. Improvement of protective devices, to make them less sensitive to distortions

2. Improvement of instrument transformers, to make them more accurate in delivering signal replicas

The second approach has resulted in so-called novel instrument transformer designs. They are based on major advance in instrument transformer technology: optical sensing of currents and voltages [4]. Optical instrument transformers are referred to as transducers. In theory, transducers have promising near-perfect performance, virtually without signal distortions. In practice, small number of currently installed transducers does not allow for making definite conclusions, whether the new technology is required for improved protection relay operation, and whether it is justifiable to replace conventional instrument transformers with transducers.

As stated above, the introduction of transducers is giving rise to a new problem: uncertainty whether the new technology needs to replace the existing one to achieve better overall relaying system. Following questions summarize this uncertainty:

1. What is the difference in performance between conventional instrument transformers and transducers ?

2. How the impact of this difference can be practically measured or evaluated ?

This thesis will make an attempt at giving answers to these questions. First, existing approaches to the problem study will be reviewed.

C. Existing Approaches to the Problem Study

Two main approaches toward the problem study can be identified in the available literature:

1. Evaluation of instrument transformer response [5], [6],[7], [8], [9], [10], [11], [12]
2. Evaluation of performance of protective devices [13], [14], [15], [16], [17], [18], [19], [20]

Neither of the approaches offers a solution that readily gives answers to the two questions posed in the section B. However, they offer initial assessment of the problem that can be further explored.

First approach, evaluation of instrument transformer response, is based on examining instrument transformer designs, as well as performance characteristics. Often the objective of the approach is to derive models, that can be used in various power system studies. The reasons for this is that traditionally instrument transformers were modelled as ideal components in the past. Models, that are available in recently published literature, accurately capture phenomena that may lead to signal distortions. However, the scope of this approach does not include impact of mentioned phenomena on performance of protective devices.

Second approach, evaluation of protection performance, is based on testing protective devices, in order to verify their correct operation for different power system conditions. Testing procedures usually focus on determining selectivity and operational time for various different disturbances and faults [21], [10], [13]. This approach does not address impact of signal distortions.

This thesis will propose a different approach to study the problem. The new approach can be regarded as synthesis of the mentioned two approaches. It assumes an evaluation of influence of instrument transformers on protection system performance by combining results from the mentioned two approaches into a systematic methodology. To better appreciate the new approach, thesis objectives will be discussed next.

D. Thesis Objectives

Objectives of the thesis are:

1. Development of a new methodology for evaluation

2. Implementation of the methodology

3. Methodology application

Steps for reaching the objective are:

- Reviewing instrument transformer designs and characteristics and their impact on signal distortions

- Analyzing protection system sensitivity to signal distortions

- Defining new and improved criteria and methodology for evaluation of influence of signal distortions on protection system

- Implementing methodology through modelling and simulation

- Applying methodology using simulation environment

E. Thesis Contribution

This thesis makes both theoretical and practical contribution toward the problem solution. Theoretical contribution is a new methodology for evaluation of influence of instrument transformers, as discussed in the previous section. The new evaluation methodology alleviates shortcomings of existing practices. It provides answers to the following questions:

- Why the evaluation of influence of instrument transformers on protection system performance is necessary and important ?

- How the influence of instrument transformers performance can be identified ?
- What are the means for quantifying (measuring) the influence ?
- What is the best procedure for coming up with quantitative measure of the influence ?
- What is the meaning of the quantitative measures ?

Practical aspect of the contribution is the development of the *simulation environment* for automated and comprehensive evaluation of the mentioned influence. The environment improves the existing evaluation practices. It allows one to derive quantitative measures of the influence indicators. Finally, it will be shown how the quantitative measures can be interpreted.

F. Conclusion

This thesis explores influence of instrument transformers on the power system protection, analyzes possible consequences and demonstrates how a new methodology can enhance existing evaluation practices. The new methodology for evaluation is defined to have the main objectives of emphasizing why the evaluation is necessary, what procedures should be applied and how to interpret the outcome of the evaluation.

The conclusion from studying the present status of the existing solutions is that there is a lot of room for improvement. The improvement need is facilitated by emerging novel instrument transformer designs (such as optical instrument transformers). The novel designs should be verified for correct supply of current and voltage signal replicas before being commissioned.

The following approach to the rest of the study in this thesis was defined: first, characteristics of instrument transformers will be discussed, as well as mechanism of their influence on the signal distortions. The protection system may be *sensitive* to mentioned distortions. This sensitivity will be investigated next. After the necessity for evaluation of the influence of distortion has been established, the criteria and methodology will be defined. A practical way of applying the methodology through software simulation will be demonstrated next. Results of the simulation will be presented.

CHAPTER II

IMPACT OF INSTRUMENT TRANSFORMERS ON SIGNAL DISTORTIONS

A. Introduction

Purpose of instrument transformers is delivery of accurate current and voltage replicas, irrespective of transformer design and characteristics. However, this is not always achieved with conventional instrument transformers. Deviations of output signals from the input ones are inherent to conventional instrument transformers, due to their design and performance characteristics.

This chapter provides theoretical background on various instrument transformer designs, performance characteristics and their impacts on output signals. Typical instrument transformer designs will be described first. Next, three most notable instrument transformer performance characteristics, accuracy, frequency bandwidth and transient response will be investigated. Their impact on signal distortions will be discussed. Illustrations of typical signal distortions will be given.

Material presented in this chapter will establish reasons why conventional instrument transformers should be improved. The material will also serve as basis for studying sensitivity of protective devices in Chapter III and for deriving evaluation criteria in Chapter IV.

B. Typical Instrument Transformer Designs

1. Current Transformers

There are two types of current transformers (CT) available: bushing and wound [1], [22], as shown in Fig. 1. The core of a bushing transformer is annular, while the secondary winding is insulated from the core. The secondary winding is permanently

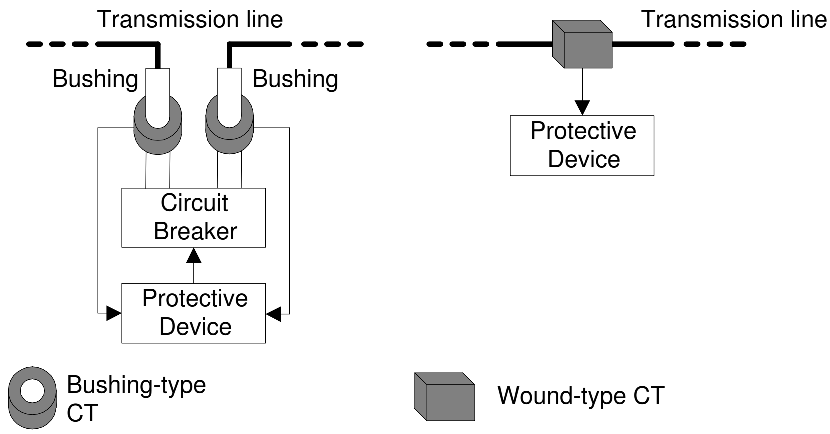

Fig. 1. Two types of current transformers

assembled on the core. There is no primary winding. The primary winding of wound transformer consists of several turns that encircle the core. More than one core may be present. The primary windings and secondary windings are insulated from each other and from the core. They are assembled as an integral structure.

Bushing transformers have lower accuracy than the wound ones, but they are less expensive [1]. Because of this favorable low-cost they are very often used with IEDs performing protection functions. Similarly, because of their great accuracy with low currents, wound transformers are usually applied in metering and similar applications. Another benefit of bushing transformers is their convenient placement in the bushings of power transformers and circuit breakers. This means that they take up no appreciable space in the substation.

The core of bushing transformers encompasses the conductor carrying the primary current. Because of such a design, the core presents relatively large path for the establishment of electromagnetic (EM) field, necessary for the conversion of current. This is the primary reason for their lower accuracy, when compared with wound transformers. However, bushing transformers are also built with increased cross-sectional area of iron in the core. The advantage of this is higher accuracy in scaling of fault currents that are of large multiples of nominal current, when compared to wound transformers. High accuracy for high fault currents is desirable in protective relaying. Therefore, the bushing transformers are a good choice for protective applications.

2. Voltage Transformers

Voltage transformers are available in two types [1]:

1. Electromagnetic voltage transformer (VT)

2. Coupling-capacitor voltage transformer (CCVT)

Voltage transformer is very similar to conventional power transformer. Main difference is that voltage transformer is connected to a small and constant load. CCVT has two main designs: 1) the coupling-capacitor device, 2) bushing device. The first design consists of a series of capacitors (arranged in a stack), where the secondary of the transformer is taken from the last capacitor in series (called auxiliary capacitor). The second design uses capacitance bushings to produce secondary voltage at the output.

In order to better understand the operating principle of a CCVT, equivalent circuit of a coupling-capacitor transformer is shown in Fig. 2 (Z_B presents the transformer burden). The equivalent reactance of this circuit can be expressed as:

$$X_L = \frac{X_{C1} \cdot X_{C2}}{X_{C1} + X_{C2}} \tag{2.1}$$

By choosing values for X_{C1} and X_{C2}, reactance X_L can be adjusted. The purpose of adjusting this reactance is to ensure that primary and the secondary voltages are in

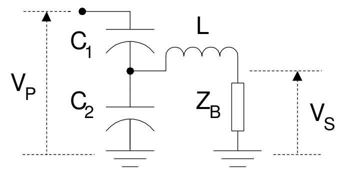

Fig. 2. Equivalent circuit of a CCVT (simplified)

phase (synchronized). Since CCVTs are built in such a way that:

$$X_{C1} << X_{C2} \tag{2.2}$$

it follows that practically

$$X_L \cong X_{C2} \tag{2.3}$$

Main purpose of coupling-capacitor transformers reduction of the transmission-level voltage V_P (primary side voltage) to a safe metering level V_S (secondary side voltage). However, an electromagnetic transformer is sometimes used in connection with the CCVT to further reduce the voltage, usually to level of 67 V line-to-neutral (115 V line-to-line).

C. Accuracy

Accuracy is a characteristic defined only for steady-state input signal, be that normal or abnormal (faulted) state. There are two accuracy rating classes for instrument transformers defined in the IEEE standard [22]. This IEEE standard is widely accepted, by both instrument transformer manufacturers and users. Therefore, it will be used as basis for discussion of accuracy. Mentioned accuracy classes are:

1. Revenue metering class

2. Relaying class

While revenue metering class is defined for both current transformers and voltage transformers, relaying accuracy class is defined for current transformers only. Both classes will be discussed, for the sake of completeness. Before discussing the classes, some additional terms will be defined first. The definitions of terms are based on [22]:

- *Transformer correction factor* (TCF) is the ratio of the true watts or watt-hours to the measured secondary watts or watt-hours, divided by the marked ratio. TCF is equal to the ratio correction factor multiplied by the phase angle correction factor for a specified primary circuit power factor.

- *Ratio correction factor* (RCF) is the ratio of the true ratio to the marked ratio. True ratio is the ratio of the root-mean-square (RMS) primary voltage or current to the RMS secondary voltage or current under specified conditions.

- *Phase angle correction factor* (PACF) is the ratio of the true power factor to the measured power factor. It is a function of both the phase angles of the instrument transformers and the power factor of the primary circuit being measured.

The two accuracy classes are discussed in more detail in sections to follow. Discussion is based on IEEE standard [22].

1. Revenue Metering Accuracy Class

Accuracy classes for metering and relaying application of instrument transformers differ. Metering usually demands more accurate secondary signals than relaying. Revenue metering accuracy classes require that the TCF of instrument transformers shall be within specified limits. This requirement is specified when the power factor

Table I. Standard burdens, revenue metering accuracy

Designation	R [Ω]	L [mH]	Z [Ω]	S [VA]	Power Factor
B-0.1	0.09	0.116	0.1	2.5	0.9
B-0.2	0.18	0.232	0.2	5.0	0.9
B-0.5	0.45	0.580	0.5	12.5	0.9
B-0.9	0.81	1.040	0.9	22.5	0.9
B-1.8	1.62	2.080	1.8	45.0	0.9

of load is in the range [0.6, 1.0]. Requirement is valid only under certain conditions, which are:

- In the case of current transformer, the load is a standard burden (see Table I). Range of input current magnitudes is [10%, 100%] of rated primary magnitude.
- In the case of voltage transformer, the load is any burden (in [VA]) in range from zero to the specified standard burden. Range of input voltage magnitudes is [90%, 110%] of rated primary magnitude.

The limits for TCF for the revenue metering accuracy classes are given in Table II.

2. Relaying Accuracy Class

Relaying accuracy classes put a requirement on the RCF of current transformers: RCF is not to exceed 10%. Since there are several relaying accuracy classes, they are

Table II. Standard accuracy classes for revenue metering (TCF limits)

CLASS	VT		CT			
			100% rated		10% rated	
	Min	Max	Min	Max	Min	Max
0.3	0.997	1.003	0.997	1.003	0.994	1.006
0.6	0.994	1.006	0.994	1.006	0.988	1.012
1.2	0.988	1.012	0.988	1.012	0.976	1.024

Table III. Standard burdens, relaying accuracy

Designation	**R** [Ω]	**L** [mH]	**Z** [Ω]	**S** [VA]	**Power Factor**
B-1	0.50	2.300	1.0	25.0	0.5
B-2	1.00	4.600	2.0	50.0	0.5
B-4	2.00	9.200	4.0	100.0	0.5
B-8	4.00	18.400	8.0	200.0	0.5

designated by a letter and a secondary terminal voltage rating, as follows:

1. Letter C, K, or T. Flux leakage in the core of current transformers, designated as C and K, does not influence transformer ratio. Additional feature of current transformer designated K is having a knee-point voltage at least 70% of the rated secondary voltage magnitude. Current transformer designated as T have appreciable flux leakage in the core. This leakage deteriorates transformer ratio significantly.

2. Secondary terminal voltage rating. This voltage is a maximum voltage, produced by a standard burden and input current of magnitude 20 times the rated one, that will still keep the transformer ratio from exceeding 10 % of RCF.

Standard burdens are given in Tables I and III. Rated secondary terminal voltages, associated with standard burdens, are given in Table IV.

Table IV. Secondary terminal voltages and associated standard burdens

Voltage [V]	10	20	50	100	200	400	800
Burden	B-0.1	B-0.2	B-0.5	B-1	B-2	B-4	B-8

D. Frequency Response

Frequency response can be evaluated only for linear systems. In general, instrument transformers are not linear devices. However, instrument transformers are usually properly sized (with parameters of various components) to operate only in linear region. This means that most of the time, instrument transformers can be regarded as linear devices. Frequency response in such cases is discussed in following sections.

1. Current Transformers

Magnitude of the frequency response of a typical current transformer is constant over a very wide frequency range (up to 50 kHz) [7]. The phase angle is also constant and has zero value. For practical purposes current transformer can be regarded as having no impact on the spectral content of the input signal, under condition that electromagnetic flux in the core is in the linear region. In case the flux goes out of the linear region, transformers are no longer considered linear devices, which means that frequency response cannot be evaluated. This situation is discussed in section E of this chapter.

2. Voltage Transformers

Similarly as in the case of current transformers, frequency response of voltage transformers and CCVTs can be evaluated only when the magnetic flux in the core is in the linear region. Cases of flux being in the non-linear region are discussed in Section E of this chapter.

Typical frequency range of signals used by IEDs is up to 10 kHz. In this range, voltage transformer frequency response acts as a low-pass filter. The cut-off frequency depends on the parameters of voltage transformer. Most notable parameters (that

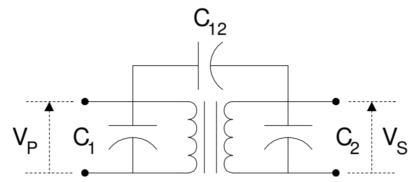

Fig. 3. Stray capacitances in a voltage transformer

influence cut-off frequency) are:

1. Stray capacitances associated with primary and secondary winding (C_1 and C_2, respectively)

2. Stray capacitance between primary and secondary windings (C_{12}).

Stray capacitances C_1, C_2, C_{12} are shown in Fig. 3, where V_P is the primary side voltage (transmission line side), V_S is secondary side voltage (IED side).

Frequency response of a typical voltage transformer can be studied using models and simulation software, such as Alternative Transient Program (ATP) [23]. The mentioned software (discussed more in chapters to come) offers frequency analysis of the models. Special benefit of using ATP is graphical user interface, available in the form of (separate) program ATPDraw. A typical ATP implementation (through ATPDraw) of a VT model is shown in Fig. 4. In the figure, generator is modelled as AC type source. Transformer is modelled as a single-phase saturable transformer. Resistors are set to value of 1 Ω, while label "V" denotes voltage probe element (voltmeter). The frequency of a typical voltage transformer obtained using the mentioned model is shown in Fig. 5. ATP can also be used for evaluation of influence of voltage transformer parameters on frequency response. The same simulation approach (as the one shown in Fig. 4) can be used for evaluation. However, such evaluation is beyond

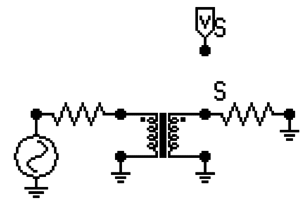

Fig. 4. Evaluation of the voltage transformer frequency response

the scope of this thesis. More on experimental evaluation of frequency response of voltage transformers can be found in reference [7].

CCVT frequency response also shows fluctuations. Most notable sources of this frequency dependability are the same as with voltage transformers. As in the case of voltage transformers, frequency response of CCVTs can be evaluated using ATP. ATP implementation (through ATPDraw) shown in Fig. 6 can be used for the evaluation.

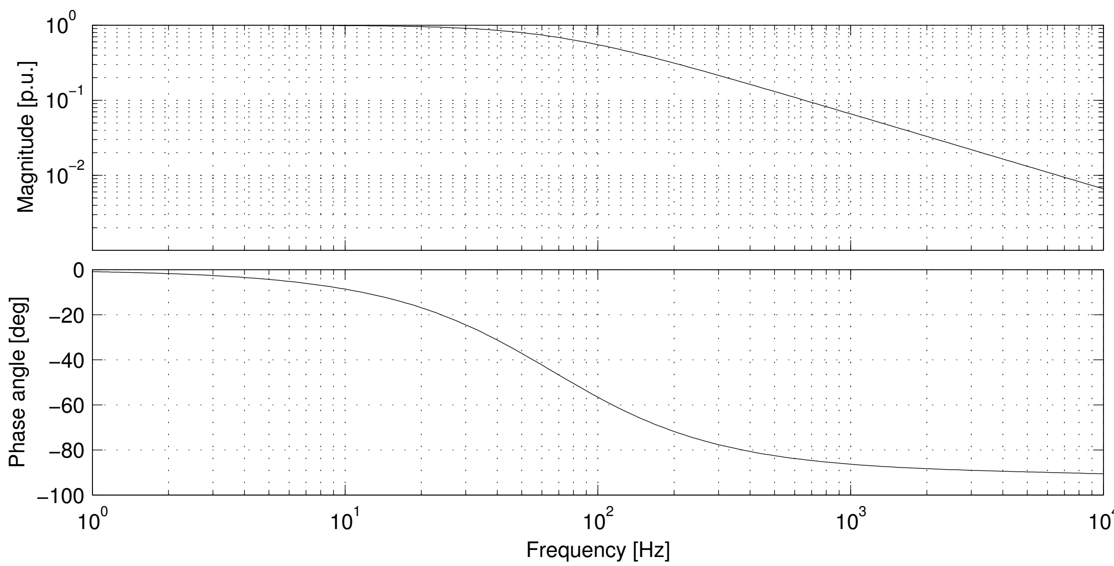

Fig. 5. Frequency response of a voltage transformer in the linear region

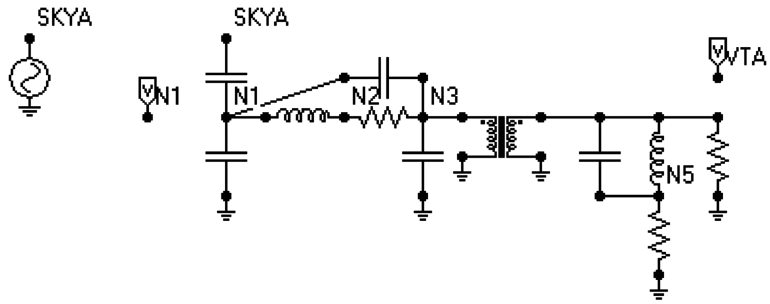

Fig. 6. Evaluation of the CCVT frequency response

In Fig. 6 various labels denote respective nodes, while value of the components (such as resistors, capacitors, etc.) are discussed in more details in Chapter V. Typical frequency response is shown in Fig. 7. More on experimental evaluation of frequency response of CCVTs can be found in reference [9].

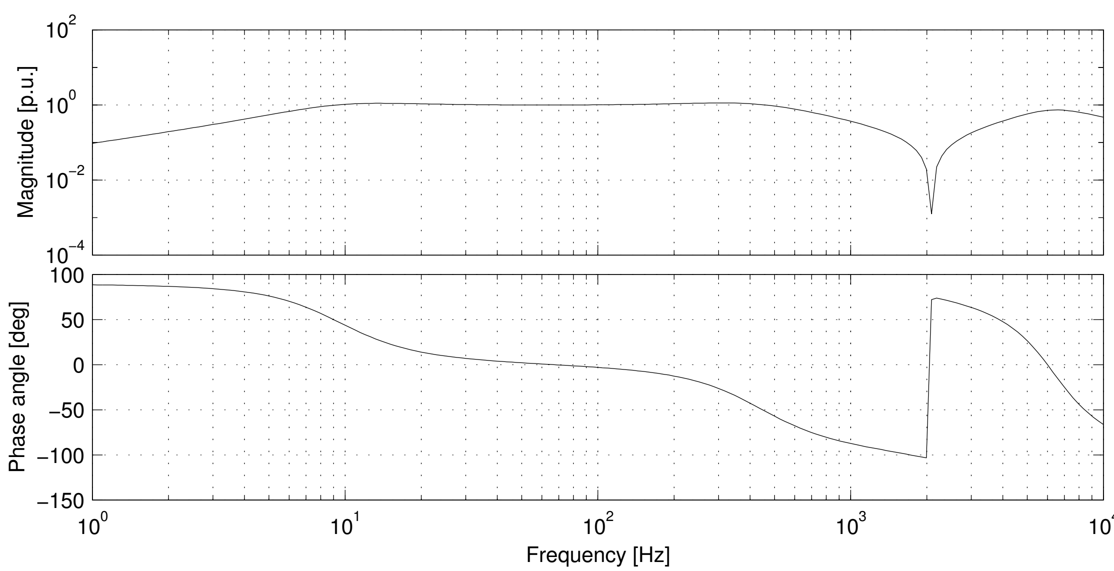

Fig. 7. Frequency response of a CCVT in the linear region

E. Transient Response

1. Current Transformers

Saturation of the electromagnetic core is the single factor that influences the current transformer transient response the most [2], [5]. It is caused by non-linear nature of the electromagnetic core of the current transformer. Saturation can lead to severe signal distortions in the current transformer output. Distortion occurs whenever the core flux density enters the region of saturation. This region can be represented using V-I characteristic of the core. A typical V-I characteristic is shown in Fig. 8. This characteristic presents dependence of exciting voltage V_E on the exciting current I_E [22]. This dependence is actually the input-output characteristic of a non-linear inductor, that can be used to model the electromagnetic core. The simplified model of the core is shown in Fig. 9.

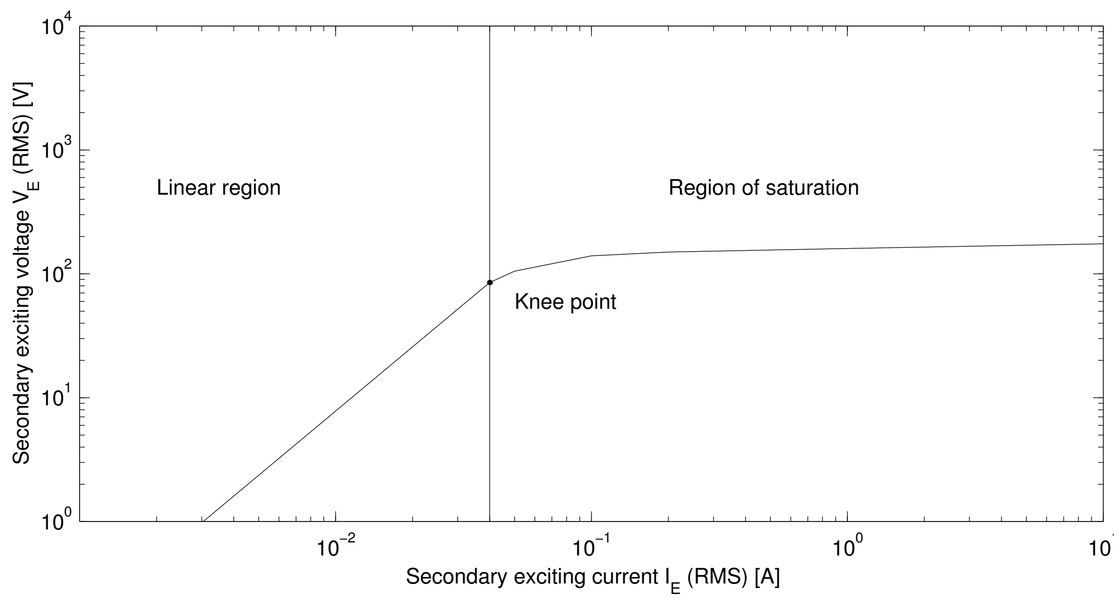

Fig. 8. V-I characteristic of the electromagnetic core

Typical power system conditions that can initiate current transformer saturation include excessive fault currents and lower magnitude asymmetrical (offset) fault currents. Major factors that affect density of the core flux are [5]:

- Physical parameters of the current transformer (transformer ratio, saturation curve, etc.)
- Magnitude, duration and shape of the primary current signal
- Magnitude and nature (active, reactive) of the secondary burden

The fault current with maximum DC offset is shown in Fig. 10. When a current transformer is exposed to this current on its input, it will induce core flux density as shown in Fig. 10 (assuming resistive burden, without loss of generality).

There are two components of the total flux Φ. Alternating flux Φ_{AC} is the flux induced by the fundamental frequency component of the fault current. Transient flux Φ_{DC} is the flux induced by the DC component of the fault current. The variation of the transient flux Φ_{DC} is a function of time constants, of both the primary and the secondary circuit. The primary circuit constant is defined by the power network section, to which the current transformer is connected. The secondary circuit time constant is defined by:

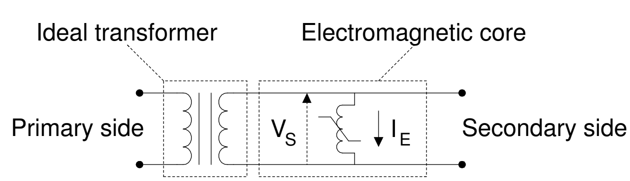

Fig. 9. Model of the transformer electromagnetic core (simplified)

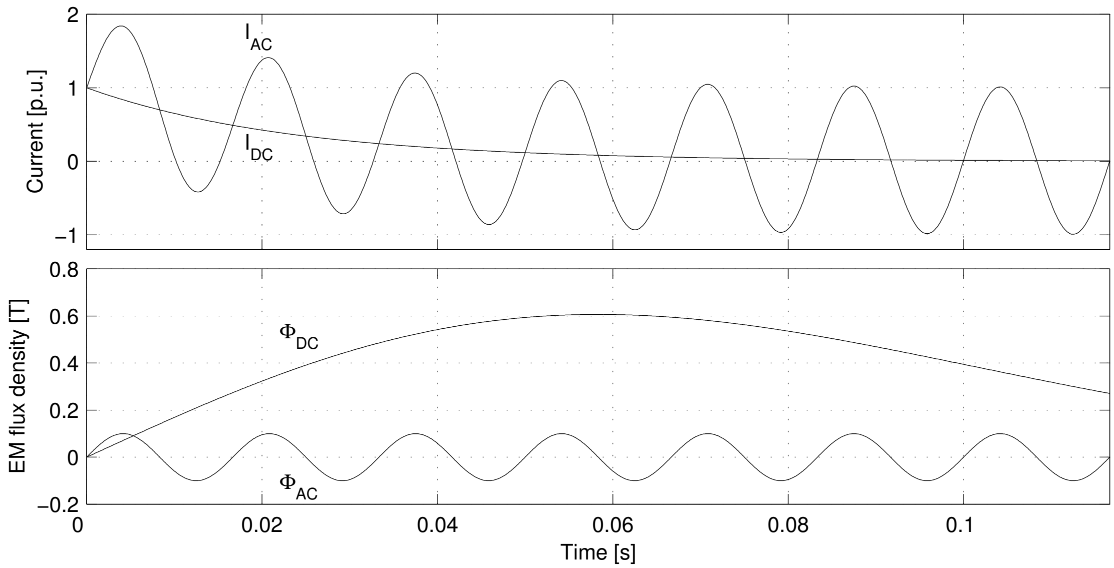

Fig. 10. Primary current and electromagnetic flux density in the core

1. Current transformer secondary leakage impedance
2. Current transformer secondary winding impedance
3. Burden impedance

The current transformer secondary leakage impedance can usually be neglected and the current transformer secondary winding impedance is usually combined with the burden impedance to form the total burden.

The dependence of the level of the saturation on the total burden is shown in Fig. 11. The figure presents comparison between the secondary (marked 1 in the figure) and the primary (referred to the secondary, marked 2) current of a 900:5 current transformer subjected to a fully offset current of 16200 A (18 times the rated value). Burden in the first case (upper diagram) is $Z_{B1} = 1.33 + j0.175\Omega$, while in the second case (lower diagram), the burden is $Z_{B2} = 8.33 + j0.175\Omega$. These two

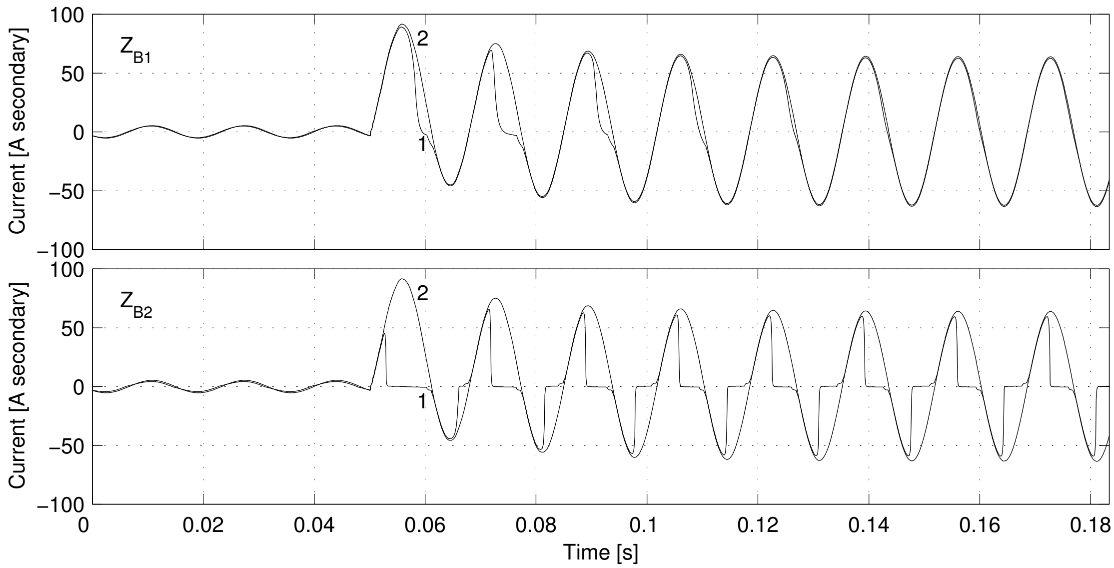

Fig. 11. Secondary current and primary scaled to secondary during a fault

burdens correspond to effect of standard burdens B-1 and B-8 (see Table III).

It can be seen in Fig. 11 that distortion begins certain amount of time after the fault inception. The notion of the *time-to-saturation* is introduced as a measure of the mentioned amount of time [5]. *Time-to-saturation* is defined as the time period, starting after the fault inception, during which the secondary current is a faithful replica of the primary current. Time-to-saturation can be determined analytically, given power system parameters. A more practical approach is to generate a set of generalized curves, that can be used for direct reading of time-to-saturation. A set of such curves can be found in [5]. Time-to-saturation is easily read from the mentioned curves by choosing the proper curve, based on the saturation factor K_s. This factor can be calculated as:

$$K_s = \frac{V_x N_2}{I_1 R_2} = \frac{\omega T_1 T_2}{T_1 - T_2}\left(e^{-\frac{t}{T_2}} - e^{-\frac{t}{T_1}}\right) + 1 \tag{2.4}$$

where V_x is RMS saturation voltage, N_2 is the number of the secondary windings, I_1 is the primary current magnitude, R_2 is the resistance of total secondary burden (winding plus external resistance), ω is $2\pi \cdot 60$ rad.

2. Voltage Transformers

There are two power system conditions that can cause problematic response of voltage transformers. The conditions are [9]:

1. Sudden decrease of voltage at the transformer terminals (due to e.g. a fault close to voltage transformer)
2. Sudden overvoltages (on the sound phases due to e.g. line-to-ground faults elsewhere in the power network)

First type of condition can produce internal oscillations within the electromagnetic core of electromagnetic voltage transformers. They appear on the secondary winding output in the form of high-frequency oscillations (frequency much higher than the system frequency, sometimes called ringing). The damping time of such oscillations is usually between 15 and 20 ms. In case of CCVTs, oscillations at the secondary winding, caused by the energy stored in the capacitive and inductive elements of the device, can last up to 100 ms. Second type of power system condition can lead to saturation of the electromagnetic core. The mechanism and effect of the saturation of the core is the same as with current transformers (which was already discussed).

The mentioned oscillations are commonly referred to as the subsidence transient. The subsidence transient generated by CCVTs is studied in reference [6]. In the study, subsidence transient is defined as an error voltage appearing at the output terminals of a coupling-capacitor voltage transformer resulting from a sudden and significant

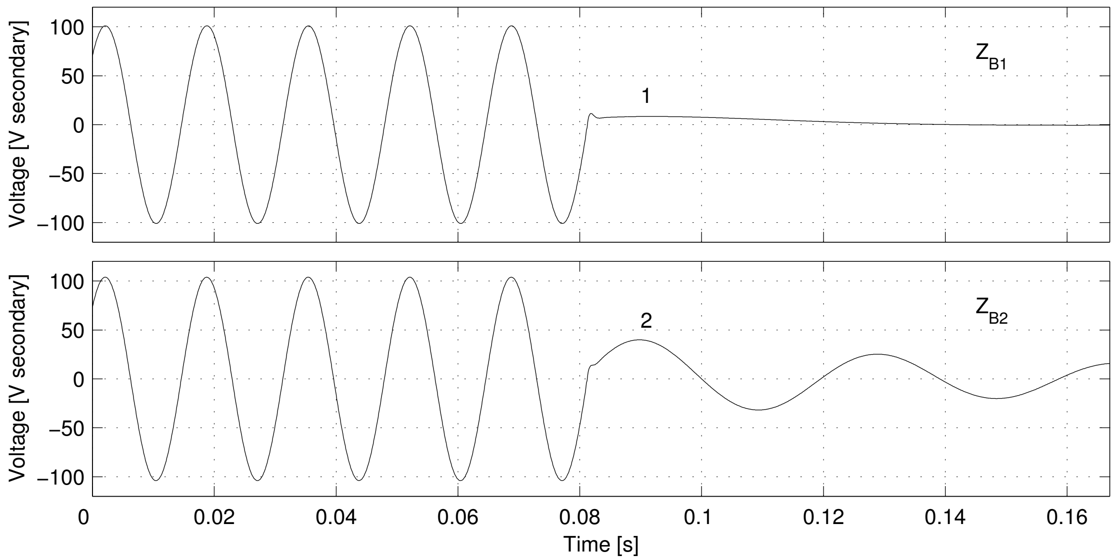

Fig. 12. Examples of a CCVT subsidence transient

drop in the primary voltage. The transient can be classified as belonging to one of the three classes:

1. Unidirectional

2. Oscillatory, $f_{oscillation} > 60Hz$

3. Oscillatory, $f_{oscillation} < 60Hz$

Examples of subsidence transients are shown in Fig. 12. Figure shows secondary voltage of a 345 kV CCVT after voltage collapse (e.g. due to a phase-to-ground fault, close to the bus containing the voltage transformer). Transients are marked 1 and 2 in the figure. Burden in case of transient 1 is $Z_{B1} = 100\Omega$ (resistive), while transient 2 is caused by burden $Z_{B2} = j100\Omega$ (inductive). The transient starts at approximately 80 ms (see Fig. 12).

The factors that influence the subsidence transient the most are:

1. Coupling-capacitor voltage transformer burden

2. Coupling-capacitor voltage transformer design

3. Ferroresonance suppression circuit (FSC)

The influence of FSC on transient response of voltage transformers will be explained in the text to follow. Experimental evaluation shows that elements of the coupling-capacitor voltage transformer burden, that influence the subsidence transient, are [6]:

1. Burden magnitude. The influence of the burden is lessened when the magnitude of the used burden is smaller than the nominal one.

2. Burden power factor. Decrease in the power factor leads to lessening of the subsidence transient.

3. Composition and connection of the burden. If there are inductive elements present in the CCVT that have a high Q factor, the subsidence transient becomes great. However, the subsidence can be lessened by using series RL burden. The subsidence transient is affected by surge capacitors in a minor way.

Coupling-capacitor voltage transformers may also contain a ferroresonance suppression circuit (FSC) connected on the secondary side [24]. Due to their design, FSC may impact CCVT transient response in certain cases. FSC designs, according to their status during the transformer operation, can be divided into two main operational modes:

- Active mode. This mode is achieved by connecting capacitors and iron core inductors in parallel, at the secondary. The mentioned elements are tuned to the fundamental frequency. Usually, such a construction is permanently placed on the secondary side.

- Passive mode. This mode of operation is achieved by connecting only a resistor at the secondary. Optionally, a gap or an electronic circuit can be placed in series with the resistor. These elements are activated whenever an over voltage occurs. Such a configuration has no effect on the voltage transformer transient response in case there is no overvoltage.

F. Conclusion

This chapter reviewed typical instrument transformer designs, their characteristics and their impacts on signals distortions. Typical current transformer designs - bushing and wound, as well as typical VT/CCVT designs were described from the standpoint of protection system. Advantages and disadvantages of some designs over other designs were addressed.

Three most notable instrument transformer characteristics - accuracy, frequency response and transient response, were investigated. It was shown that all three characteristics can lead to distortions. Main source of distortions with current transformers is the saturation. Main source of distortions with VTs/CCVTs is the subsidence transient and ferroresonance. Causes and mechanisms of mentioned distortions were discussed. Means of lessening their impact were also addressed.

The conclusion is that impact of instrument transformer designs and characteristics on distortions may be significant. When the power system conditions are adequate, output signal can be significantly different from the scaled-down version of input signal. This presents motivation to investigate influence of distortions on protective devices. This issue is addressed in the next chapter.

CHAPTER III

PROTECTION SYSTEM SENSITIVITY TO SIGNAL DISTORTIONS

A. Introduction

Algorithms inside protective devices are designed to achieve maximum selectivity and minimum operational time for fault waveforms as inputs. Algorithm performance in case of artificial deviations from such input signals is hard to predict. Depending on type and extent of deviation, protective devices might be "fooled" into making wrong decisions, such as unnecessarily isolating network sections, or failing to disconnect faulted component.

This chapter analyzes sensitivity of protection system to artificial distortions in current and voltage signals on input. Core of protection system are IEDs - Intelligent Electronic Devices. Their elements and functions are described first. Next, the mentioned sensitivity is established using a simple test method. Finally, negative impacts of distortions are investigated. Material in this chapter demonstrates the necessity for evaluation of influence of signal distortions.

B. Elements and Functions of the Power System Protection

Functions of modern protection systems are performed by IEDs. Typical elements of IEDs are shown in Fig. 13. The elements are arranged to make measurements and decision regarding interpretation of observed variables (current, voltages, power flow, etc.), as well as take action as required.

Elements in Fig. 13 may be complex, consisting of sub-elements. Data acquisition block is the front end that performs filtering, sampling and digitalization of the analog input current and/or voltage signals. Measuring block extracts desired quantities,

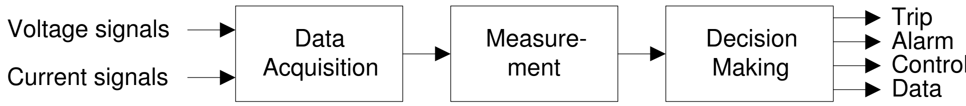

Fig. 13. Functional elements of a typical IED

such as current and voltage phasors, impedance, power, etc. Signal processing and decision making block relies on basic operating principles to derive trip, alarm, control or data signal. The flowchart of the decision making block is shown in Fig. 14.

Decision making element constantly compares the measured quantities, or some combination of them, against a threshold setting that is computed by the protection engineer and is entered into the IED. If this comparison indicates an alert condition, a decision element is triggered. This may involve a timing element or some other checks on signals coming from other relays. Finally, if all the checks lead to a conclusion that there is a fault, an action element is enabled to operate. This operation is the actual execution of a trip by a protection function. Basic protections functions include:

- Overcurrent protection: A function that operates when its input (current) exceeds a predetermined value

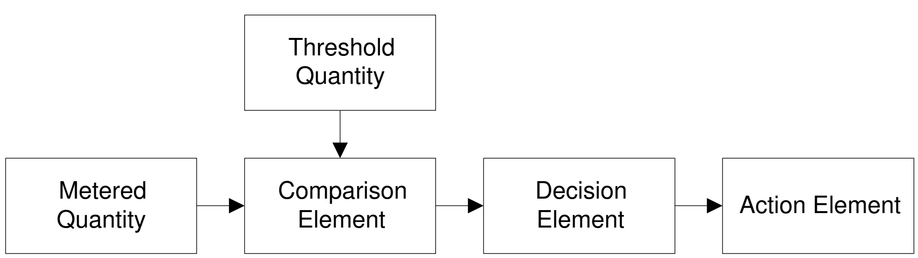

Fig. 14. Flowchart of the decision making block

- Directional protection: A function that picks up for faults in one direction, and is restrained for faults in the other direction

- Differential protection: A function that is intended to respond to a difference between incoming and outgoing electrical quantities associated with the protected apparatus

- Distance protection: A function used for protection of transmission lines whose response to the input quantities is primarily a function of the electrical distance between the relay location and the fault point

- Pilot protection: A function that is a form of the transmission line protection that uses a communication channel as the means of comparing relay actions at the line terminals

C. Types of Signal Distortions

Possible conditions of a power system can be divided in two general categories:

1. Normal condition

2. Abnormal (faulted) condition

Power systems often carry signals that are corrupted in one way of another, irrespective of the condition. Dominant distortions in normal condition are power quality (PQ) disturbances. There are several different definitions of PQ disturbances in the literature [25].

Distortions that are dominant in abnormal (faulted) condition are transients. Transient are phenomena caused by power system's inability to instantaneously transfer energy, due to presence of energy-storing components, such as inductor and capacitor banks.

This thesis will address protection system sensitivity only to signals belonging to the second category, abnormal (faulted) condition.

Field application has shown that instrument transformers do not cause significant signal distortions during normal power condition, while they may induce severe distortions during abnormal conditions (see Chapter II). General explanation for such a performance is as follows:

- Instrument transformers are designed with normal conditions in mind. This means that components of the design (such as electromagnetic core, various capacitors, inductors, etc.) are chosen to operate in linear regions, when exposed to signals up to certain magnitudes (component ratings). Disturbances in normal operation do not cause these elements to leave linear region of operation [5], [6], [8], [9]. In order to properly size (select) mentioned transformer components, study has to be performed, to calculate maximum operating current under all expected disturbances, such as harmonic components, power quality events, and similar.

- During abnormal (faulted) conditions, current and voltage magnitudes can change rapidly (within fractions of a 60 Hz cycle), in the range of thousands of volts and amperes. If the change of signal magnitudes is sufficient (in current power systems it often is), instrument transformers will be moved out of linear region of operation.

D. Protection Function Sensitivity to Signal Distortions

A simple method can be used to establish IED sensitivity to input signal distortions. The method proposed here covers typical distortions caused by instrument transformers (see Chapter II). However, any kind of distortion can be evaluated for impact on

IEDs.

The method can be summarized as follows: IED sensitivity can be checked by comparing IED response (output) when exposed to different levels of distortions in the same input signal. This approach can be found in literature [26], [27].

The method can be illustrated by sensitivity of overcurrent protection IED to current transformer saturation. A simple simulation was carried out on models of current transformers and IEDs. Results are shown in Fig. 15. In order to generate signals with different levels of saturation, two current transformer models were used for scaling-down of primary side signals. Difference between models is the V-I characteristic of the electromagnetic core. The two characteristics are discussed in Chapter V. IED input signals produced by the two current transformers (shown in Fig. 15) show different levels of distortion. Output signals of IED models show the same response for both input signals. However, when burden of the second current transformer was increased from $Z_{B1} = 1.33 + j0.175\Omega$ to $Z_{B2} = 8.33 + j0.175\Omega$, IED model showed significantly different response, also shown in Fig. 15. Conclusion is that IED model is sensitive to distortion levels above a certain threshold. Questions that arise from the conclusion are:

1. Are there negative impacts of distortions on IED performance, or can they be neglected ? (i.e. is IED sensitivity significant enough to cause undesirably low performance)

2. If there is negative impact, how can it be measured ?

The first question is discussed in the following section. The second question is dealt with in the next chapter.

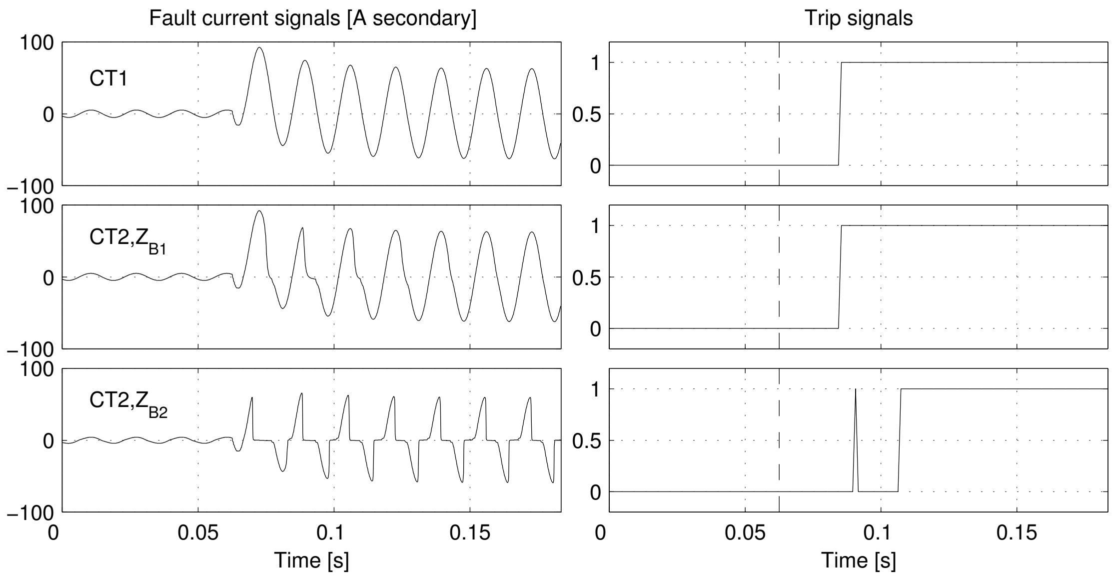

Fig. 15. Examples of the IED sensitivity to input signal distortions

E. Negative Impact of Distortions

1. Impact of Current Transformers

Negative influence of distortions was reported in the literature. There are studies that investigate the impact of various distortions on different protective functions [26]-[28]. Study [26] investigates some specific applications, when it is expected that current transformers will saturate during asymmetrical faults (situations such as unplanned extension of the current transformer wiring cable, which greatly increases its burden). Most protection devices make operating decisions based on the RMS[1] value of fault current. If the signal supplied by the current transformer is distorted by saturation, the RMS values calculated by the protection device will be lower than the RMS values of the actual fault current. In the case of overcurrent protection, this can

[1]RMS: Root Mean Square

cause protection device to trip with undesired delay.

In order to verify these results, simulation was performed using models of a saturable current transformer and an overcurrent protection relay (details of the mentioned models can be found in references [9], [29]). Simulation was carried out to evaluate impact of current transformer saturation. A phase-A-to-ground (AG) fault was simulated at 10% of the transmission line length at 0.05 s. The phase A fault current (including a portion of the pre-fault steady state) is shown in Fig. 16. The dotted line represents the primary current scaled to secondary, while the full line represents the secondary current, which is supplied to the relay model. Fig. 16 also shows the trip signal derived by the relay model (dotted line presents trip signal for the undistorted input signal, while the full line presents trip signal for input distorted by saturation). Fig. 16 shows delayed tripping (more than one 60 Hz cycle). The delay is long enough that it may present threat to safe operation of the entire power system.

Work presented in reference [30] addresses impact of current transformers on the distance protection. The results show that when the current transformer undergoes distortion, the measuring algorithm detects the fundamental frequency component of the fault current with a lower value than the actual. This kind of distortion can make the calculated impedance trajectory to enter and exit the zone of protection before the trip signal is asserted, or the calculated trajectory may not enter the zone of protection during the first cycle in which the fault occurred. Therefore, the effect of the current transformer saturation can cause a delay in issuing a trip signal. It should be noted that if the current transformer undergoes saturation by the symmetrical fault current (i.e. when the exponential decay component is zero) the impedance trajectory calculated by the measuring algorithm may never enter the zone of protection.

To verify the results from [30] simulation was performed using models of a sat-

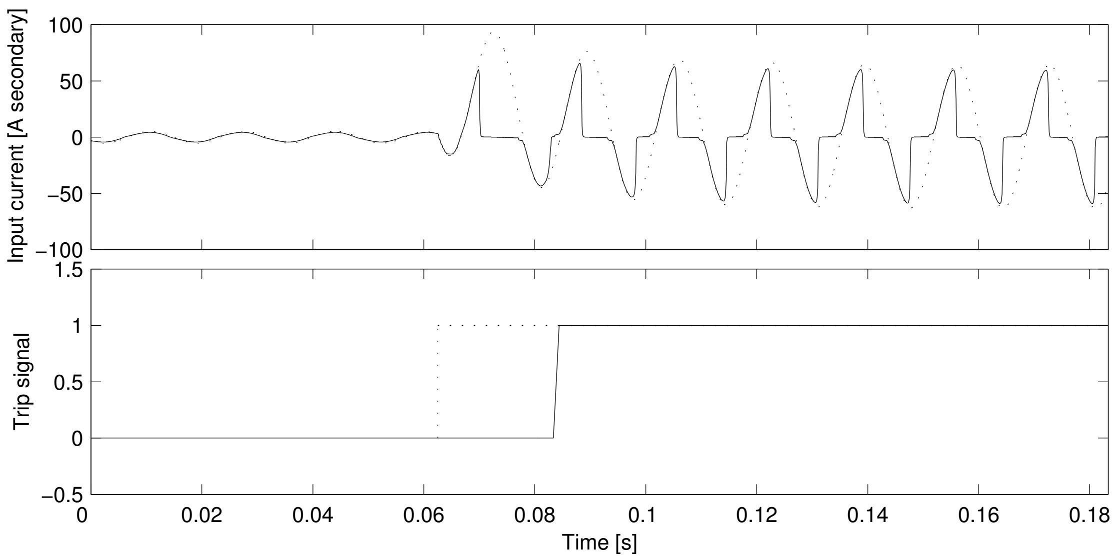

Fig. 16. Input current and the relay model response for a simulated fault

urable current transformer, a saturable CCVT and a distance protection relay (details of the mentioned models can be found in references [9], [29]). Simulation was carried out to evaluate impact of current transformer saturation. A phase-A-to-ground (AG) fault was simulated at 75% of the transmission line length. The reach of the zone 1 protection was set at 80% of the line length, while the reach of the zone 2 was set at 120% of the transmission line length. The R-X impedance plane is suitable for visualizing the calculation of the fault impedance by the relay model. R-X impedance plane is organized by a two-axis coordinate system, where abscissa represents real part of the impedance, i.e. $\Re\{Z\}$ and ordinate represents imaginary part of the impedance, i.e. $\Im\{Z\}$. Fault impedance trajectories are shown in R-X plane in Fig. 17. Fig. 17 contains trajectories calculated from undistorted and distorted input current and voltage signals, where numbers 3 through 8 represent sample instances after the fault inception (impedance is calculated for every sample of input current

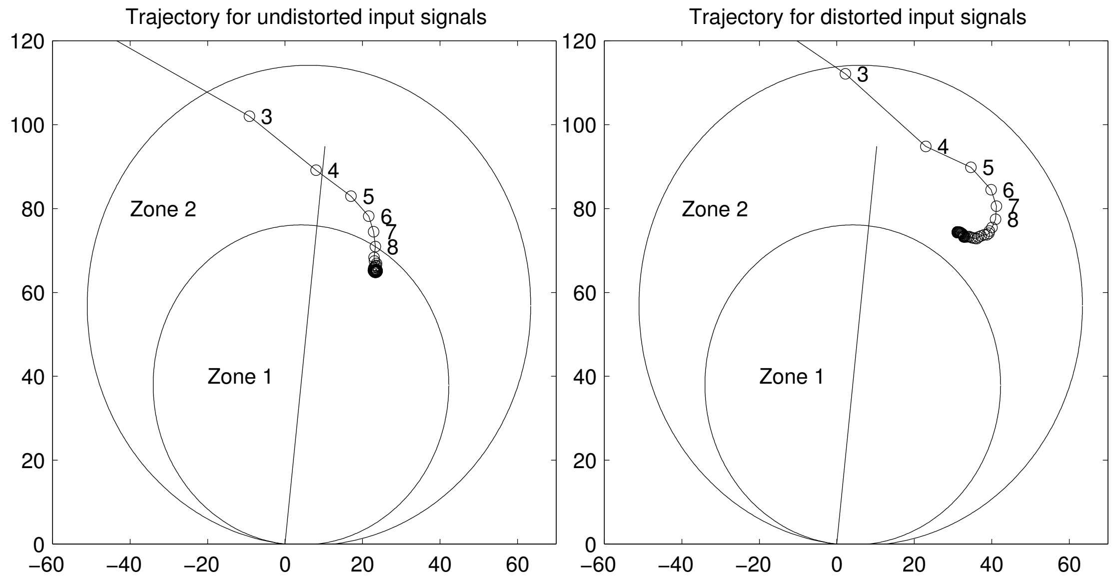

Fig. 17. Fault impedance trajectories (CT impact evaluation)

and voltage signals). In this illustration, the measuring algorithm has sampling rate of eight samples per cycle, and has sampling resolution of sixteen bits (every sample is presented as sixteen-bit number). The undistorted input signals are shown in Fig. 18, while distorted input signals are shown in Fig. 19. Differences between undistorted and distorted input current signals, ΔI_A, ΔI_B, ΔI_C, are shown in Fig. 20, to better display the distortions.

Fig. 17 shows that fault was identified within zone 1 during the first 60 Hz cycle after the fault inception for undistorted input signals, while the relay model miss-operated by detecting a fault in zone 2, and asserted only an intentionally-delayed trip signal (relay acted only as a backup protection) for distorted input signals. The relay model response in this case was unexpected. Such behavior clearly demonstrates negative impact of distortions caused by current transformers.

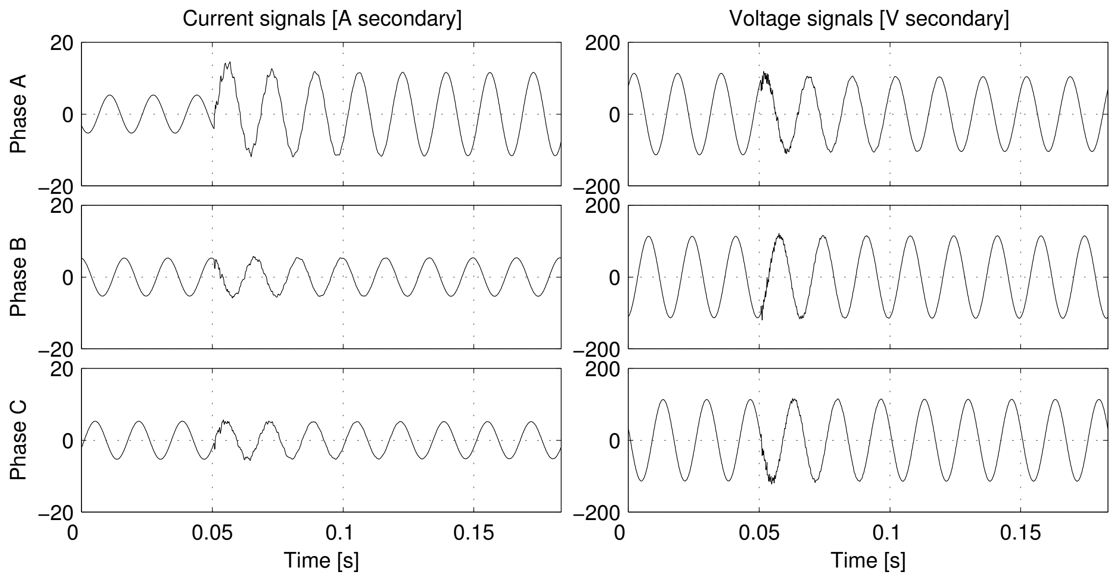

Fig. 18. Undistorted input signals (CT impact evaluation)

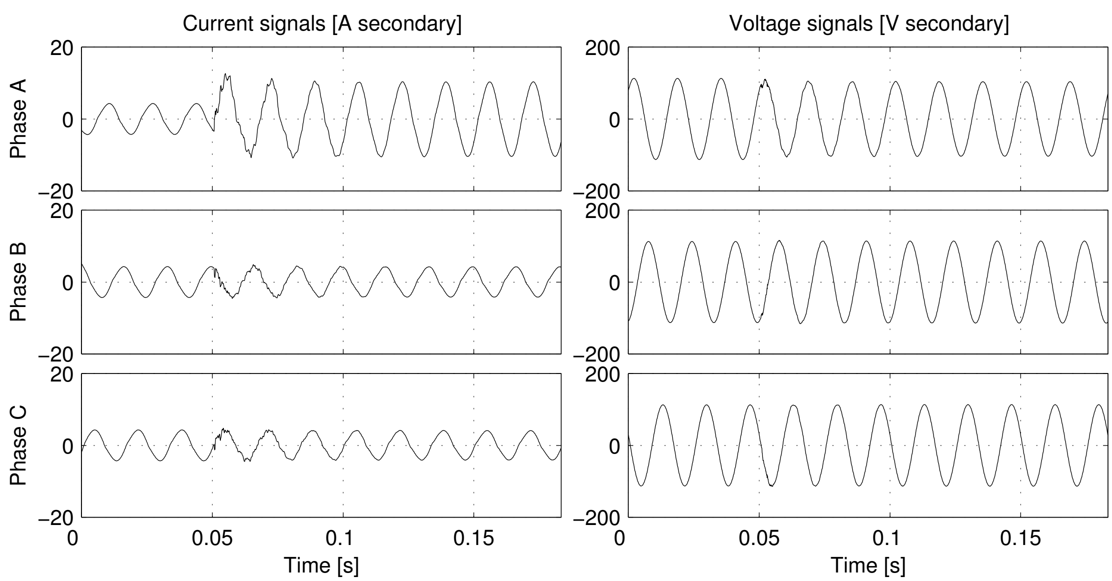

Fig. 19. Distorted input signals (CT impact evaluation)

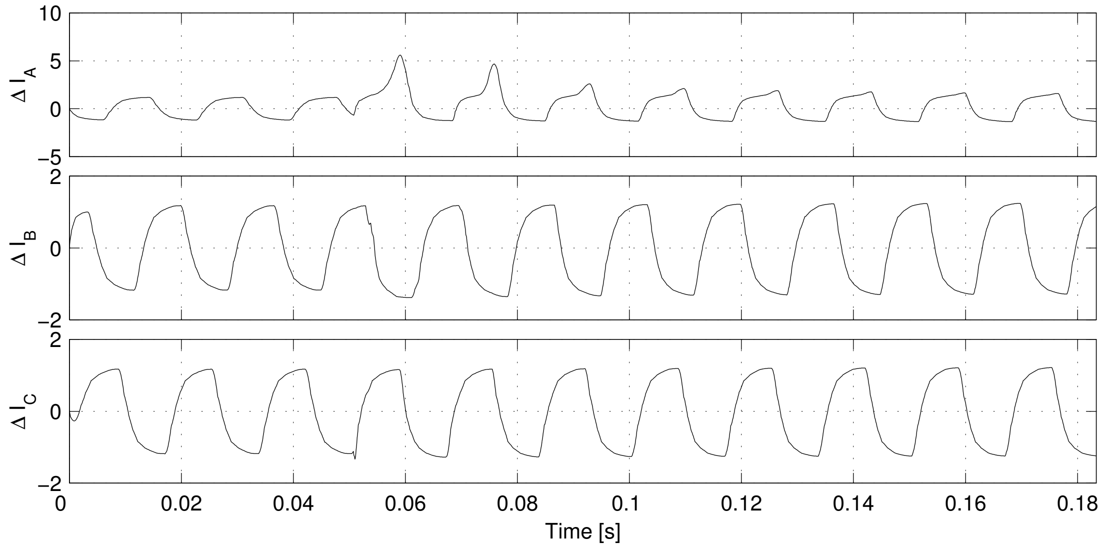

Fig. 20. Difference between undistorted and distorted input current signals

2. Impact of Voltage Transformers/CCVTs

Studies [27] and [28] examine impact of voltage transformer and CCVT on the distance protection. The results are showing that error, generated by the voltage transformers, is often large, compared with the primary signal (being measured) and with the sensitivity of connected IEDs. In the case of a distortion, the IED performance may be degraded and one-cycle operation may not be possible any more.

To verify results from [27] and [28], simulation was performed using models of a saturable current transformer, a saturable CCVT and a distance protection relay (details of the mentioned models can be found in references [9], [29]). Simulation was carried out to evaluate impact of voltage transformer saturation and subsidence transient. A phase-B-to-phase-C fault was simulated at 85% of the transmission line length. The reach of the zone 1 protection was set at 80% of the line length, while the reach of the zone 2 was set at 120% of the transmission line length. Fault impedance trajectories are shown in Fig. 21. Fig. 21 contains trajectories calculated from undistorted and distorted input current and voltage signals, where numbers 5 through 11 represent sample instances after the fault inception (impedance is calculated for every sample of input current and voltage signals). In this illustration, the measuring algorithm has sampling rate of eight samples per cycles, and has sampling resolution of sixteen bits (every sample is presented as sixteen-bit number).

As can be seen, the trajectory indicates fault impedance within zone 2 for instances 5,6,7,8. Fault impedance for instances 9,10,11 is in a critical vicinity of the border line between zones 1 and 2. This critical vicinity is showed in more detail in Fig. 22. Fig. 22 shows that fault impedance enters zone 1 only during one instance for undistorted input signals, while the fault impedance remains in zone 1 during two instances for distorted input signals. This additional instance of fault impedance being in zone 1 is caused by CCVT-induced distortion. The relay model correctly operated when supplied with undistorted input signals (relay model intentionally delayed trip assertion). The relay model miss-operated when supplied with distorted input signals (relay model immediately asserted trip, as if the fault impedance was in zone 1). Undistorted input signals are shown in Fig. 23, while distorted input signals are shown in Fig. 24. Since it is virtually impossible to identify the difference between the Figs. 23 and 24, differences between undistorted and distorted input voltage signals ΔV_A, ΔV_B, ΔV_C are shown in Fig. 25.

The difference between trajectories shown in Fig. 22 shows that IED models can be very sensitive to input signal distortions. This kind of sensitivity is dependent on the design of the protective IEDs. The distance relaying algorithm involves counters which monitor the number of calculation iterations for which the impedance remains within a certain zone of protection. Depending on the threshold settings of the counters, protection may or may not be sensitive to certain input signal distortions.

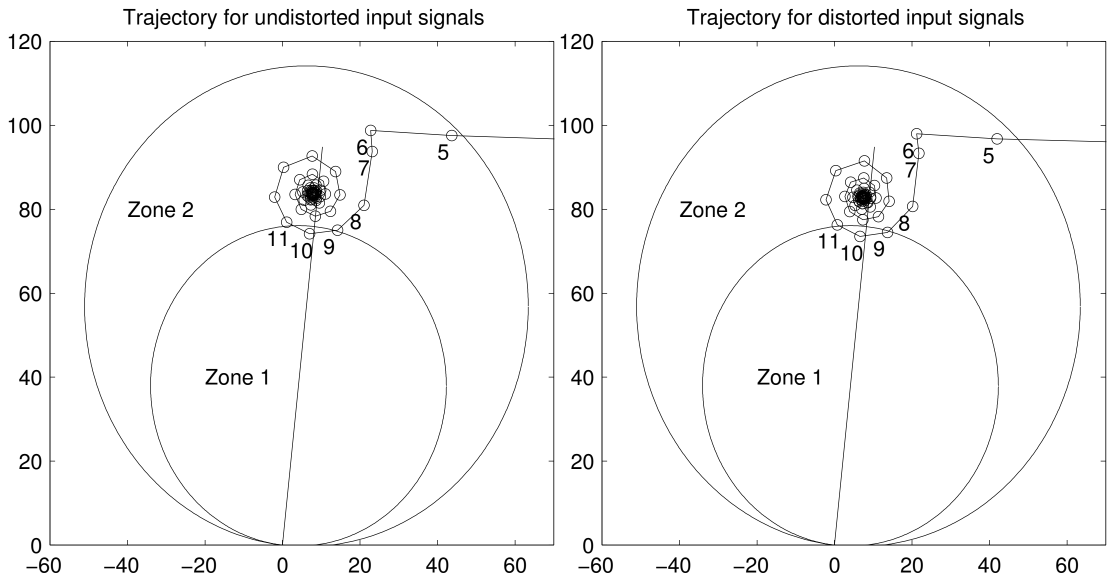

Fig. 21. Fault impedance trajectories (VT impact evaluation)

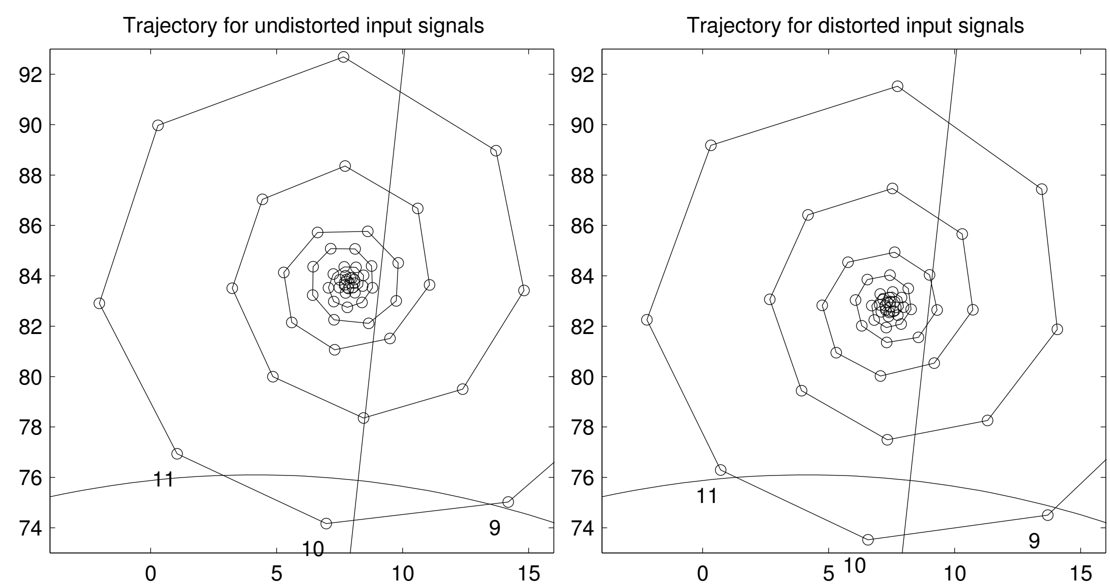

Fig. 22. Enlarged portions of fault impedance trajectories (VT impact evaluation)

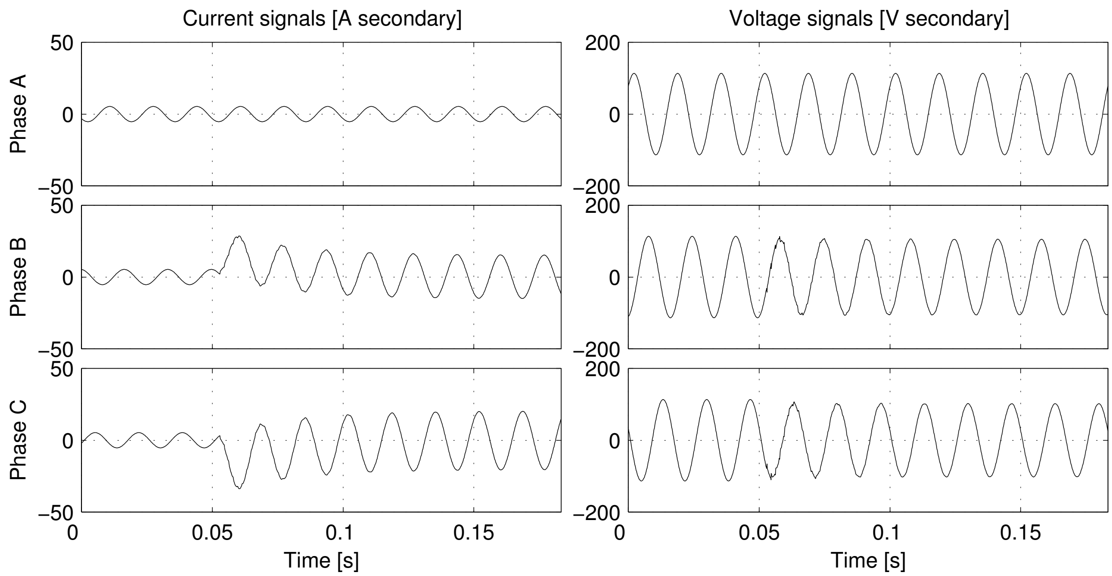

Fig. 23. Undistorted input signals (VT impact evaluation)

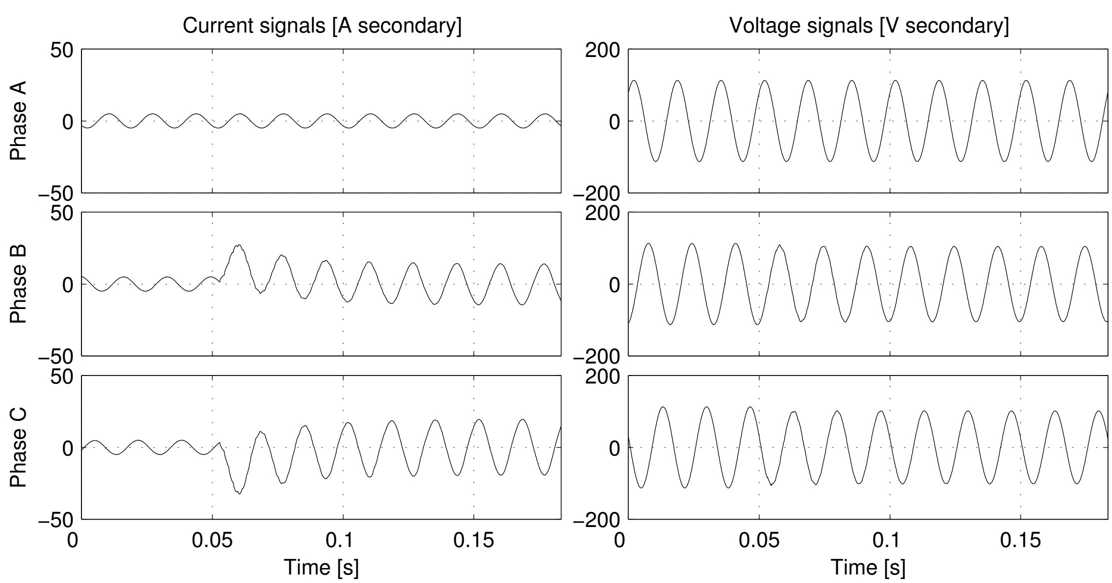

Fig. 24. Distorted input signals (VT impact evaluation)

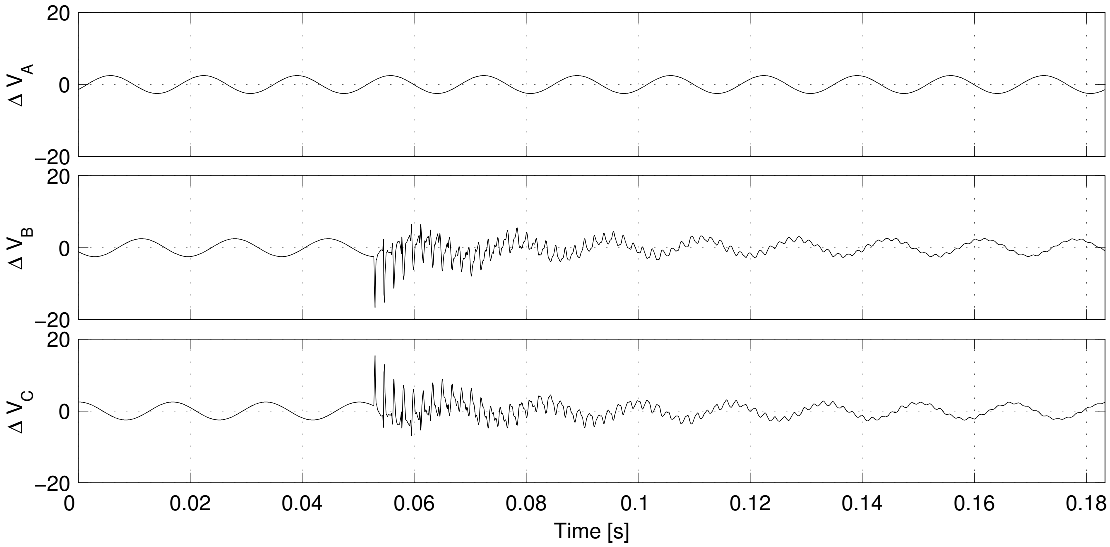

Fig. 25. Difference between undistorted and distorted input voltage signals

F. Cause of Protection Sensitivity to Signal Distortions

Test cases from the previous section have shown that even the small changes in input current and voltage signals can lead to misoperation of protective relays. The cause of this sensitivity of protection relays is the nature of response of protective relays to input signals.

Studies of performance evaluation of the protection system have shown that the procedure for derivation of the trip signal for steady-state input signals is deterministic, while for transient input signals the the procedure is *stochastic* [13], [14], [15], [16]. An illustration of this stochastic nature is the analysis presented in reference [13]. Trip decision is based on a certain parameter (derived from input current and voltage signals), which can be denoted as $Z(t)$. The mentioned parameter has the value $Z_{prefault}$ during the steady-state preceding the fault inception, and it has the value $Z_{postfault}$ during steady-state following the fault inception (the two mentioned steady-state periods are separated by a transient period). During the transient period associated with the fault, the discrete-time representation of the parameter $Z(t)$ can be written as:

$$Z(n) = Z_{prefault} + S(n) \tag{3.1}$$

where n is index of a time point, $S(n)$ is the error of the estimated value. Ideally $S(n) = 0$ for every n. Since ideal conditions are hardly met in practical application of relays, it is necessary to minimize discrete signal $S(n)$. One of the minimization techniques commonly used is minimum square error minimization. The objective of this technique is to find $\min(E\{S^2(n)\})$ under the constraint $E\{S(n)\} = 0$, where $E\{x\}$ denotes expected value of the ensemble of signals. In practice, this technique is applied through simulation of many test cases and subsequent statistical analysis of signals $Z(n)$. The time-average value Z_k^N of the signal $Z(n)$ during the test case number k can be expressed as:

$$Z_k^N = \frac{1}{N} \sum_{n=1}^{N} Z(n) \tag{3.2}$$

where N is the number of time-points during which the time-average is calculated. For total number K of test cases, mean value M of signals $Z(n)$ can be expressed as:

$$M = \frac{1}{K} \sum_{k=1}^{K} Z_k^N \tag{3.3}$$

In case there was no estimation error, the condition $E\{M - Z_{postfault}\} = 0$ would be valid. Since this situation is hardly a case in practical application of relays, index R can be used as a measure of the randomness of response of protective relays:

$$R = |M - Z_{postfault}| \tag{3.4}$$

G. Conclusion

The material covered in this chapter explained the sensitivity of the protection system to signal distortions. First, basic elements and functions of the protection system were described. It was shown that protection system is complex, both in elements and functions. A simple method was used to demonstrate sensitivity of IEDs to distortions. Since sensitivity varies depending on the amount of distortion, possible negative impacts were discussed and illustrated. The primary cause of sensitivity of protection system to input signal distortions was explained (random nature of the protection system response).

The conclusion of the chapter is that protection system is sensitive to signal distortions. This sensitivity is not negligible. It was shown that signal distortion may lead to protection misoperation, such as delayed trips and failures to trip. Therefore, *methodology for evaluation of the mentioned influence is necessary, in order to correctly identify all situations that could lead to unacceptable protection response.*

This conclusion presents incentive for development of a methodology for the mentioned evaluation. This methodology, as well as associated criteria, is dealt with in the next chapter.

CHAPTER IV

EVALUATION OF THE INFLUENCE OF SIGNAL DISTORTIONS

A. Introduction

Evaluation of relay performance is necessary in order to properly identify all the situations when protection system may miss-operate, operate with unacceptably low selectivity or unacceptably long operational time. This identification can help prevent possible future misoperations. Other benefits of the mentioned evaluation include overall improvement of protection schemes.

This chapter defines a set of criteria that can be used for numerical evaluation of the protection system performance. Numerical evaluation means that criteria is expressed quantitatively. Measuring and decision making algorithm are separate elements of protection IEDs (see Chapter III). Therefore, criteria for the mentioned algorithms is defined separately.

A new methodology for evaluation is also defined in this chapter. The definition is summarized by answers to several crucial questions. Main contribution of the new methodology is the combined approach to the evaluation. Currently, methodologies for performance evaluation of instrument transformers and the protection system exist. The new methodology, presented here, combines the mentioned two types of methodologies, to evaluate the impact of instrument transformers on protection system performance.

B. Shortcomings of the Existing Performance Criteria

Currently, there are many informal criteria that categorize the response of protection IEDs. A typical criteria (that can be found in literature) classifies the protection operation in the following classes [2]:

1. Correct
   - As planned
   - Not as planned or expected
2. Incorrect, either failure to trip or false tripping
   - Not as planned or wanted
   - Acceptable for the particular situation
3. No conclusion

Even though such a performance characterization can be useful, it suffers from certain shortcomings:

- The classes are too broad in certain situations. For example, performances of two protection devices that both properly detected a fault, but operated with different time delays, can both be classified as correct. The are no means within the mentioned class to indicated the difference in performance between the two devices. Field experience has showed that such difference may cause miss-coordination of the protection scheme [26].

- Classes are defined using intuitive terms, such as "planned" or "wanted". Depending on the circumstances, these terms may vary greatly (e.g. "as planned" operation may encompass a broad range of correct operations, where some of these correct operations may be bordering with incorrect operations, as in the case of overcurrent protection exposed to low-current faults that produce very long operational time). Also, in certain situations it may prove hard to clearly state limits between the terms. An example of such a situation is when a distance protection IED clears a fault near the end of zone 1, with unplanned time delay close to planned time delay for faults in zone 2.

- The classification does not give any information about the reasons why the protection system operated in a certain manner. This brings out the fact that such a scale is focused primarily on the link between the cause (fault, disturbance, etc.) and the effect (protection system response), without taking into account the processes taking places during the derivation of the protection response.

The above shortcomings make the mentioned performance criteria a poor choice for evaluation of the influence of signal distortions on protection system performance. In order to evaluate this influence accurately, a new evaluation criteria needs to be defined, that will alleviate the mentioned shortcomings.

C. Criteria Based on the Measuring Algorithm

1. Time Response

Measuring algorithm traces a specific feature of the input signal (e.g. amplitude of a sinusoidal waveform) [16]. That specific feature is called the measured value. Measured value is usually constant during the steady-state. However, transient periods of the input signal cause significant fluctuations in the measured value within very small time-intervals. Fluctuations can be illustrated by time response of a measuring algorithm. Typical time response of a measuring algorithm is shown in Fig. 26. This time response represents amplitude of a fault current signal (phase-to-ground fault), where fault (event) occurs at 0.05 s.

Objective of the measuring algorithm is to capture all measured value fluctuations with best possible accuracy. Performance indices can evaluate to what extent is this

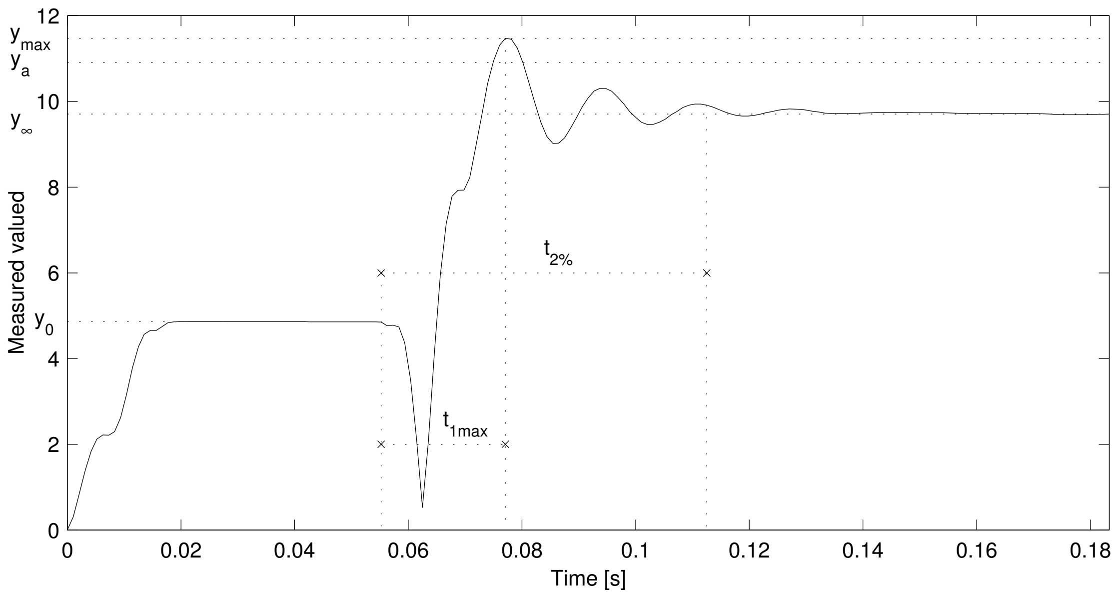

Fig. 26. Parameters of the generalized measuring algorithm time response

objective achieved. Definitions of indices (used in this thesis) are based on reference [16]. The following indices are defined as:

- Settling time, $t_{2\%}$, is a time in which the measured value reaches its steady state with the accuracy of 2% after the inception of the event. The limit accuracy can in certain cases be extended to 5%.

- Time to the first maximum, t_{1max}, is a time in which the measured value reaches its maximum value for the first time after the inception of the event.

- Overshoot, $\Delta y_{\%}$, is defined as:

$$\Delta y_{\%} = \frac{y_{max} - y_{\infty}}{y_{\infty}} \tag{4.1}$$

- Normalized error index, e_{norm}, is defined as:

$$e_{norm} = \frac{1}{M \cdot (y_{\infty} - y_0)} \sum_{k=L}^{L+M} \left(y_{(k)} - y_a\right) \tag{4.2}$$

Index e_{norm} is computed in the window of M samples starting from the L-th sample. The reasons for the use of M-sample window is that some decision making algorithms use transient monitors to postpone derivation of the output signal. This is reflected in the choice of the value of L. When transient monitor is used, performance of the measuring algorithm is of interest only after the transient period has passed. In case the influence of the transient monitor needs to be neglected, L should be set to 1.

2. Frequency Response

Measuring algorithms in protective IEDs are designed to estimate a feature of a harmonic component at specified frequency. In the United States, the frequency harmonic is 60 Hz (in Europe, it is 50 Hz). To be able to correctly identify the mentioned harmonic, other frequencies components should be suppressed during measurement. However, small variations of specified frequency (60 Hz) are possible in power systems. Because of this, measuring algorithms usually act as narrow band-pass filters.

Spectral content of a signal, with amplitude shown in Fig. 26, is given in Fig. 27. Figure contains a portion of the spectrum around 60 Hz (since this is the frequency of interest). This spectral content Y_{actual} is the frequency response of the actual measuring algorithm. Performance indices, that measure how much this response is different from the ideal (band-pass filter) response Y_{ideal} can be defined. Definitions of indices (used in this thesis) are based on reference [16]. The following indices are defined:

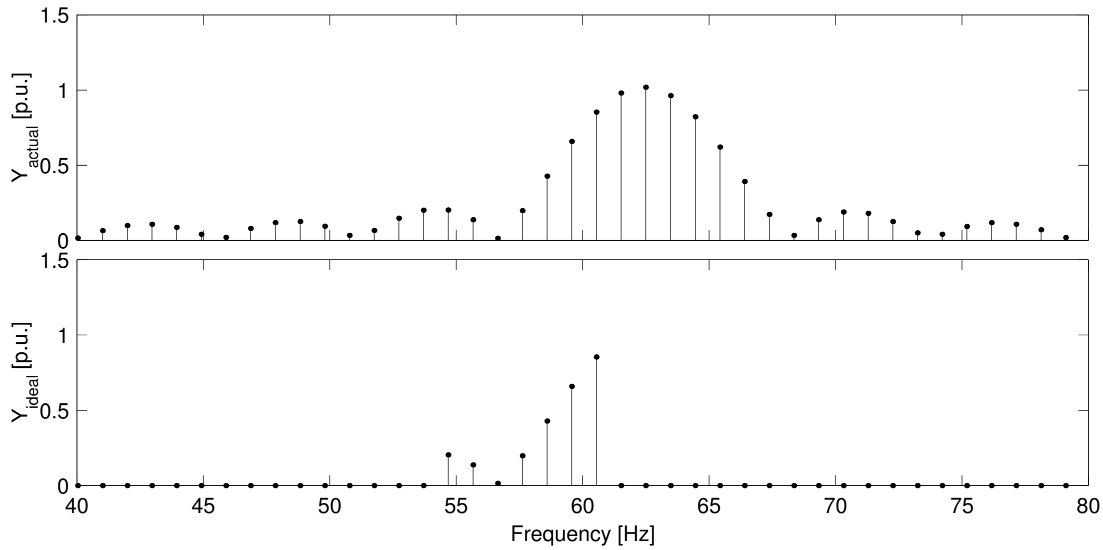

Fig. 27. Frequency response of the actual and the ideal measuring algorithm

- Gain for DC component, FR_{DC}, is defined as:

$$FR_{DC} = \frac{Y_{actual}(0)}{Y_{actual}(60)} \tag{4.3}$$

- Aggregated index F, is defined as:

$$F = \frac{1}{f_2 - f_1} \int_{f_1}^{f_2} |Y_{ideal}(f) - Y_{actual}(f)|\, df \tag{4.4}$$

Even thought indices for time and frequency response are based on reference [16], contribution of this thesis lies in software implementation of those indices and their subsequent use for evaluation of influence of instrument transformers (while in reference [16] their use is confined to evaluation of relay performance).

D. Criteria Based on the Decision Making Algorithm

Decision making algorithm is supplied with the measured signals by the measuring algorithm. By processing the measured signals, decision making algorithm derives the final output. Final output may take one of the several forms. Examples are trip signal (binary signal), fault location (numerical value) and power measurement (continuous or discrete real signal). Based on the context of the output signal, evaluation criteria for the decision making algorithm can be defined. The definitions developed in references [14], [15] are the good starting point. Extending those definitions, reference [16] proposes a more compact form of the decision making algorithm performance index:

$$J = C \cdot P_0 + (1 - C) \cdot P_1 + A \cdot t_{trip} \tag{4.5}$$

where C is an arbitrary factor defining the relative importance of the missing operations and false trippings, A is an arbitrary scaling factor defining the importance of fast reaction time, P_0,P_1 are percentages of false trippings and missing operations, respectively [14], [15], t_{trip} is the average tripping time. The lower the index J, the better the relay performance. In this thesis, a different relay performance index is defined and used:

- Selectivity, s, defined as:

  $$s = \frac{N_1 + N_0}{N} \tag{4.6}$$

  where N_1 denotes number of correct trip signals issued, N_0 denotes number of correct trip restraints and N is the total number of exposures. In ideal case $N = N_1 + N_0$.

- Average tripping time, t, defined as time between fault inception and issuing of trip signal.

E. Calculation of Performance Indices

While performance indices, defined in previous sections, may seem simple, their calculation, based on realistic signals, can be quite involved. One major issue that needs to be investigated further is the overshoot. Definition supplied in section C is valid for any input signal. However, implementation of that definition needs further clarification.

Depending on the input signal, measured value may have different shapes. Four shapes that are often found in signals from power networks are shown in Fig. 28. These four shapes are useful in illustrating calculation of the overshoot. In the figure, abscissa presents time (in [s]), while time-points where an event occurs (that leads to change of measured value) are marked with a vertical dashed line. As can be seen, measured values in Figs. 28(a) and (b) actually do not show any overshoot. In Figs. 28(c) and (d) the overshoot is present. The two overshoots differ significantly, though. In figure (c) the overshoot is result of a drop of measured value from pre-event value to post-event value. The overshoot is negative. In figure (d) the overshoot results from a rise of the measured value. This leads to a positive overshoot. Because of this overshoot behavior, it is necessary to have the means to differ between overshoot types (when calculating performance indices). Simple way of differentiating between the overshoots is to compare the pre-event and post-event measured values. In the case the pre-event is greater than the post-event value, the overshoot is found as the minimum of the measured value, after the event occurrence. If the pre-event value is smaller than the post-event, the overshoot is found as the maximum of the measured value, again, after event occurrence. Another issue is the fluctuation of steady-state value. After the 2% setting time, measured value (depending on type of measuring algorithm) often oscillates around certain value. For this reason, parameter y_{inf} (see

Fig. 26) is derived as the mean of the measured value over time, starting from moment it enters 2 % accuracy region. This is illustrated in Fig. 29. Diagram on the top shows the measured value, while Diagram in the bottom contains zoomed portion of the signal.

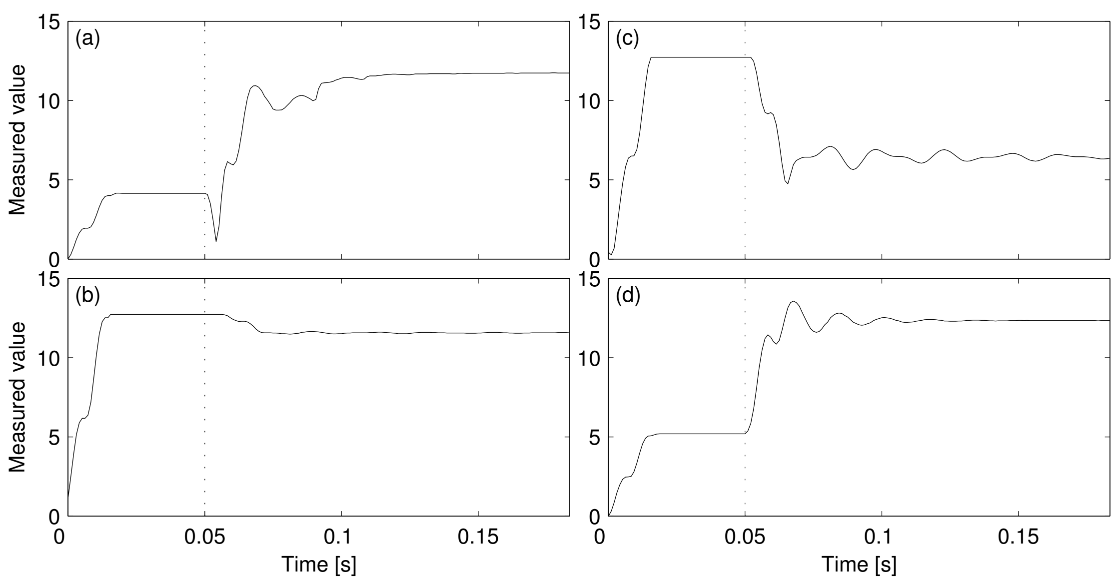

Fig. 28. Different types of overshoot

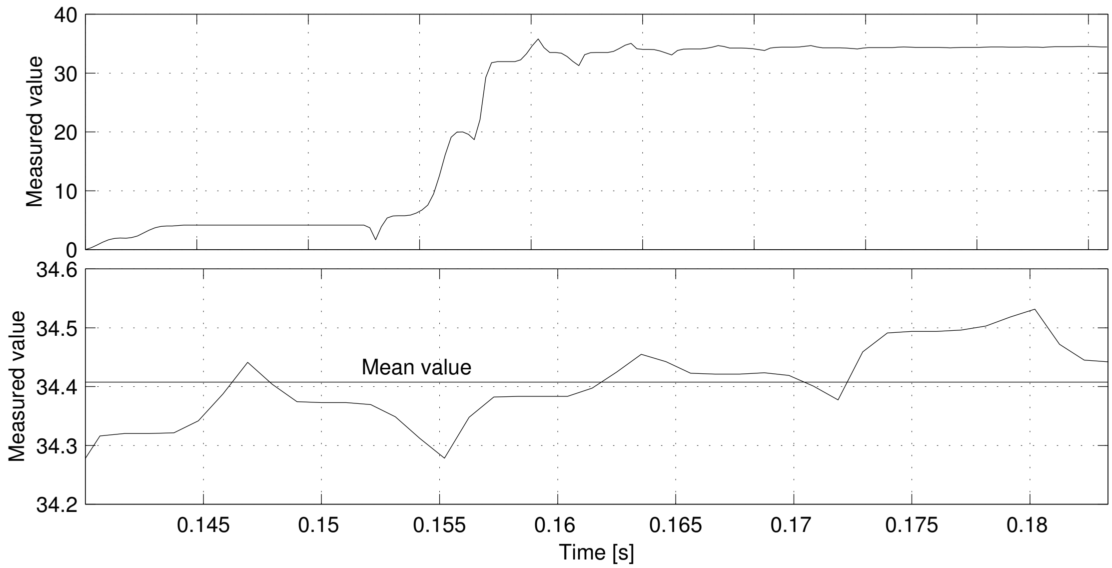

Fig. 29. Steady-state value fluctuation

F. Referent Instrument Transformer

The above indices (from both time and frequency domain) can be used to evaluate performance of the measuring algorithm. In order to measure impact of distortions on the algorithm, indices could be calculated for an algorithm first exposed to (scaled-down, undistorted) primary signals, and afterwards for an algorithm exposed to a distorted replica. In practice, this would require having available current and voltage signals from the primary side of current transformers and voltage transformers. In vast majority of installed instrument transformers, these signals are extremely hard to obtain, for one or another reason (unaccessible instrument transformer primary, high voltage and current magnitudes at the primary, etc.). In order to overcome this difficulty, a notion of a referent instrument transformer is introduced.

In order to evaluate influence of distortions caused by instrument transformers, a comparison of the index values is necessary. A difference in values of the performance indices between:

1. Measuring algorithm exposed to signals supplied by a referent instrument transformer

2. Measuring algorithm exposed to signals supplied by instrument transformer under investigation

is an indicator of the influence of a particular instrument transformer on the measuring algorithm performance. The main idea behind this concept is that referent instrument transformer can be regarded as ideal, and therefore, deliver exact signals from the primary side. This is, of course, impossible to achieve with realistic transformers. However, it may not be necessary to demand such high performance from referent instrument transformer. Referent instrument transformer can be any instrument transformer which performance has two characteristics:

1. Performance is known, meaning that it has been proven in field application or laboratory testing as accurate

2. Performance is stable, meaning that it has been proven over some period of time to be not deteriorating

An example of one such instrument transformer would be novel, optical current transducer. Its laboratory testing and preliminary field application point toward both characteristics. The meaning and the interpretation of the difference depends on the choice of the particular indices used as criteria. It is possible to choose a particular set of indices to target evaluation of influence of a particular instrument transformer characteristic. For example, if the influence of the transient response (see Chapter II) needs to be evaluated, a set of criteria indices may consist of:

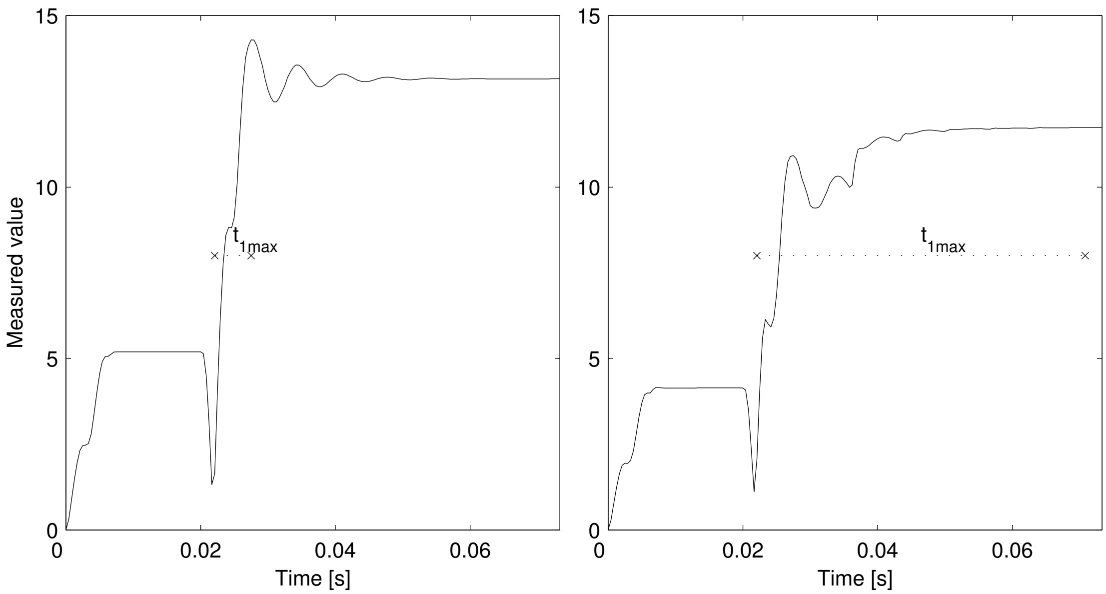

Fig. 30. Comparison of the performance index t_{1max} for undistorted and distorted input signals

1. Overshoot, $\Delta y_{\%}$

2. Time to the first maximum, t_{1max}

Tests can be conducted (by exposing the instrument transformer to various power system conditions) to calculate the values of the indices. If the saturation occurs, with the increase of the level of saturation, overshoot is expected to decrease while time to the first maximum is expected to increase, in comparison with the time response of the referent instrument transformer. This comparison is illustrated in Fig. 30. This is an example of how comparison of index values can identify increase of saturation. The mentioned targeted evaluation can be extended into a methodology, which is explained next.

G. Definition of the New Methodology

New methodology for evaluation is intended to improve existing practice. Key elements of the methodology definition are:

1. Establishing reasons why evaluation is necessary
2. Proposing criteria for evaluation
3. Defining procedure and identifying tools for evaluation
4. Interpretation of evaluation results

The key elements are summarized in the form of questions and answers.

Why is evaluation of influence of instrument transformers on IEDs necessary and important ? There are two main reasons:

1. Instrument transformers are known to distort signals coming from the primary side. At present, there is no generally successful way to altogether eliminate distortions. Main reasons for distortions are instrument transformer design characteristics, which are inherent to instrument transformers. Characteristics and their impact on distortions are discussed in the Chapter II.

2. Protection IEDs are sensitive to signal distortions. This sensitivity can, in certain cases, cause misoperation of IEDs. Since distortions originate inside instrument transformers, we can regard distortions as direct influence of instrument transformers. Negative impacts of distortions are discussed in Chapter III.

How can the influence of instrument transformers be measured ? The influence can be measured by defining criteria in a context of the protection system functions. The evaluation can be done by comparing performance of the functions in two cases:

1) functions exposed to signals supplied by a referent instrument transformer, 2) functions exposed to signals supplied by instrument transformers under investigation. Difference in numerical values of the performance indices are a clear and effective indicator of the mentioned influence. This concept of comparison is discussed in section F.

What are the means for quantifying the influence (finding numerical values) ? There are well-defined performance indices for various protection elements and functions in the literature [13]-[16]. These indices can be adapted to serve as a quantitative indicator of the influence of the instrument transformers on the protection function performance. Practical definition of the criteria, taken from [16], is given in sections C and D. It is important to note again that, index values itself are NOT an indicator of the mentioned influence; rather, the DIFFERENCE in values is the indicator.

What is the best procedure for finding the quantitative values of the instrument transformer influence ? The best procedure is a statistical analysis of the performance of the protection system. Statistical methods can be used as a tool to quickly and efficiently sort through large number of test cases, and derive values of indices. The basis of the statistical analysis methodology are available in the literature [16]. One particular statistical method will be developed later in the thesis.

What is the meaning of the quantitative values ? Quantitative values are statistical indicators of the function performance (to what extent the protection system performance was satisfactory ?). The difference in the numerical values for the cases defined in the first question is a numerical indicator of the influence of instrument transformers on the function performance.

H. Conclusion

This chapter introduced criteria for evaluation of the signal distortions on IEDs. First, the reasons for doing so were discussed. Separate criteria was defined for different elements of IEDs. It was shown how particular distortions, caused by certain instrument transformer characteristics, can be targeted for evaluation. One application of this targeting, methodology for evaluation, was also discussed.

The conclusion of the chapter is that presented criteria can be used as an effective and meaningful mean for identification of influence of distortions. The criteria is based on quantitative values, which means that evaluation is exact and comprehensive. Based on this, a new methodology for evaluation was defined. They key elements of the methodology are: 1) reasons why evaluation is necessary, 2) criteria for evaluation, 3) tools for evaluation, 4) interpretation of evaluation results. All elements were explained. It was concluded that the new methodology presents a systematic and exhaustive approach to the problem posed in the first, introductory chapter. Based on the definition of the new methodology, a simulation approach will be presented in the next chapter.

CHAPTER V

EVALUATION THROUGH MODELING AND SIMULATION

A. Introduction

The performance indices, defined in previous chapter, may be calculated by analyzing output signals of IEDs. Outputs of IEDs are triggered by certain input signals. Options for generating IED inputs to obtain output signals are:

- Field-recorded data
- Signals obtained from simulations

If the field recorded data contains all the signals necessary for calculation of performance indices, then the indices can be derived directly from the data. What are the necessary signals depends on the nature of indices. Since large number of signal cases is desirable (field recordings may not be sufficient), the simulation often proves to be a more practical approach.

This chapter describes evaluation through modelling and simulation. Simulation approach will be addressed first. Next, power network, instrument transformer, and IED models will be listed and described. The reasons for their selection will also be discussed. Afterwards, scenarios for simulations will be defined. The material presented in this chapter is a background for software implementation, presented in the next chapter.

B. Simulation Approach

As mentioned in the introduction, IED model responses are initiated by input signals derived by simulating signals corresponding to various power system events (faults, disturbances, etc.). The input signals, derived from simulating a given event, constitute a single exposure [14]. In this thesis, exposure is defined as a 3-phase set of current and voltage waveforms, that represent given power system event. An example of exposure is shown in Fig. 18 (in Chapter III). The fault for which the exposure was captured is a phase-A-to-ground (AG) fault, without phase-to-ground resistance. As can be seen in the figure, exposure contains steady-state waveforms, followed by a transient after the inception of fault. Signals, that make an exposure, trigger IED model to perform certain operations, and to issue certain output signals, if necessary. Correct IED model response may be either issuing a trip signal, or restraining from tripping.

Objective of the simulation is to subject IED models to a large number of exposures and record IED responses. Afterwards, the recorded data is used for derivation of performance indices. The simulation procedure can be summarized in the following steps :

1. Create a database of exposures by simulating events using power network model
2. Feed the exposures into the models of instrument transformers and IEDs
3. Record necessary IED output signals (from both the measuring and decision making algorithm)

The steps are illustrated in Fig. 31. Shaded elements produce output that is stored for future use. Two main elements of a simulation are:

1. Models
2. Scenarios

In the following sections, models used in simulation will be described. Importance of proper selection of models will be emphasized. Afterwards, scenarios will be defined.

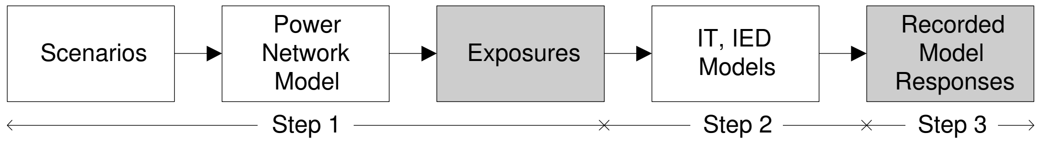

Fig. 31. Steps of the simulation procedure

C. Simulation Models

1. Power Network Model

Model of the power network should accurately capture dynamic characteristic of disturbances, including faults. Network interconnections should be included as Thevenin equivalents. Power network model selected for simulations is a 9-bus, 11-lines, 345 kV power system section. Fig. 32 shows one-line diagram of the network. The model was developed according to example given in reference [31]. The example is based on a realistic power network section.

2. Current Transformer Models

Models of instrument transformers should include features that accurately represent their characteristics, discussed in Chapter II. Four current transformer models were chosen for evaluation. All the models have the same general equivalent circuit, shown in Fig. 33. The circuit is proposed as suitable for simulation in the literature [8], [10], [26].

Differences between models are in their parameters. Parameters were chosen to be representative of current transformer characteristics that can cause distortions. Saturation, the major cause of distortion, is mainly dependent on the current transformer burden and V-I characteristic of the electromagnetic core. Therefore, two

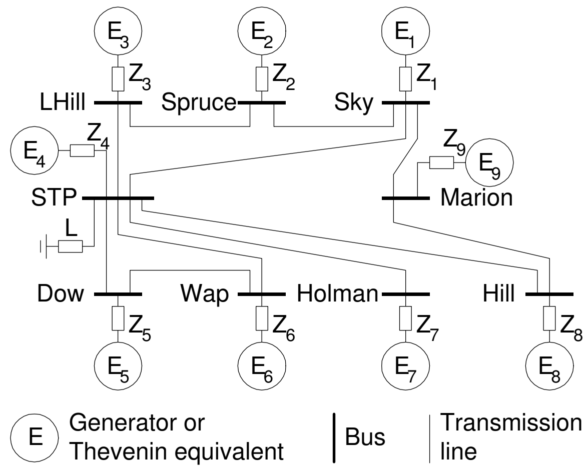

Fig. 32. Model of the power network section

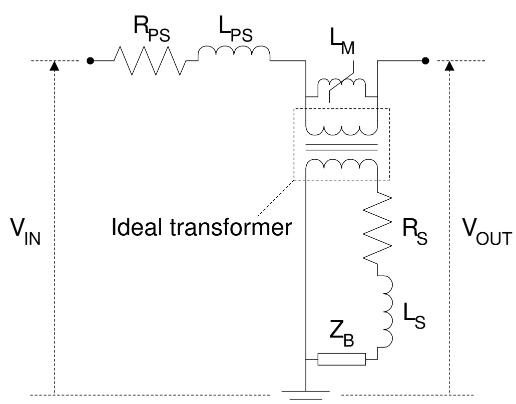

Fig. 33. Model of the current transformer

different burdens and two different V-I characteristics were chosen. Combining them gives total of four model cases. Parameter selection for models is shown in Table V. The selected burdens are $Z_{B1} = 1.33 + j0.175\Omega$ and $Z_{B2} = 8.33 + j0.175\Omega$. The magnitude of the burdens are 1.34 Ω and 8.33 Ω, which is equivalent to standard burden B-1 and B-8, defined in IEEE standard [22] (see Table III, in Chapter II). The two characteristics are shown in Fig. 34. The rest of model parameters are shown in Fig. 33.

3. CCVT Models

Choice of CCVT/voltage transformer models followed the same approach as choice of current transformer models. Since power network model used in simulations is high-voltage (HV) transmission network, CCVT was selected as an appropriate voltage-transforming device. Voltage transformer is included as a part of CCVT, as additional step-down element. Four models were chosen for evaluation. Subsidence transient, major cause of signal distortions, is dependent mainly on CCVT burden and configuration. For this reason, two different burdens and two different configurations were chosen. Parameters selection for models is shown in Table VI. Burdens are: resistive burden $Z_{B1} = 100\Omega$, and inductive burden $Z_{B2} = j100\Omega$. This choice of burden is often found in literature, when evaluating CCVT characteristics [10], [24]. The two configurations are shown in Fig. 35.

Table V. Parameters of CT models

Model	**Burden**	**Characteristic**
1	Z_{B1}	1
2	Z_{B2}	1
3	Z_{B1}	2
4	Z_{B2}	2

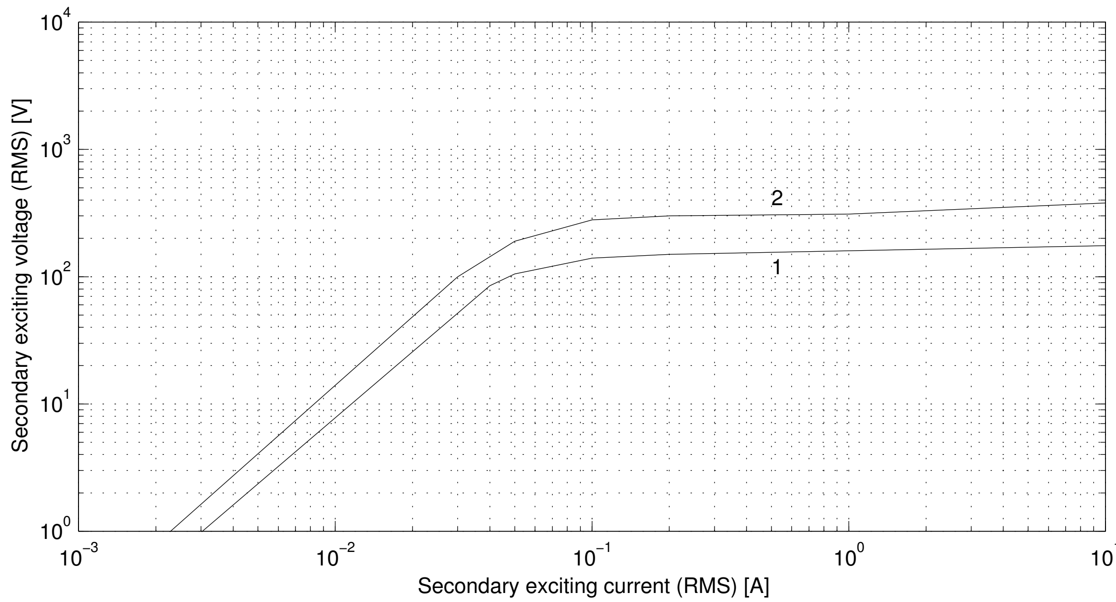

Fig. 34. V-I characteristics of the current transformer core

4. IED Models

Models of IEDs should include all the functional elements of the original IEDs. Output signals from functional elements should be available (e.g. measuring algorithm should have output available to the user - most of the readily available models in the literature do not poses this feature).

Two IED models were selected for simulations: IED model A and IED model B.

Table VI. Parameters of CCVT models

Model	**Burden**	**Configuration**
1	Z_{B1}	1
2	Z_{B2}	1
3	Z_{B1}	2
4	Z_{B2}	2

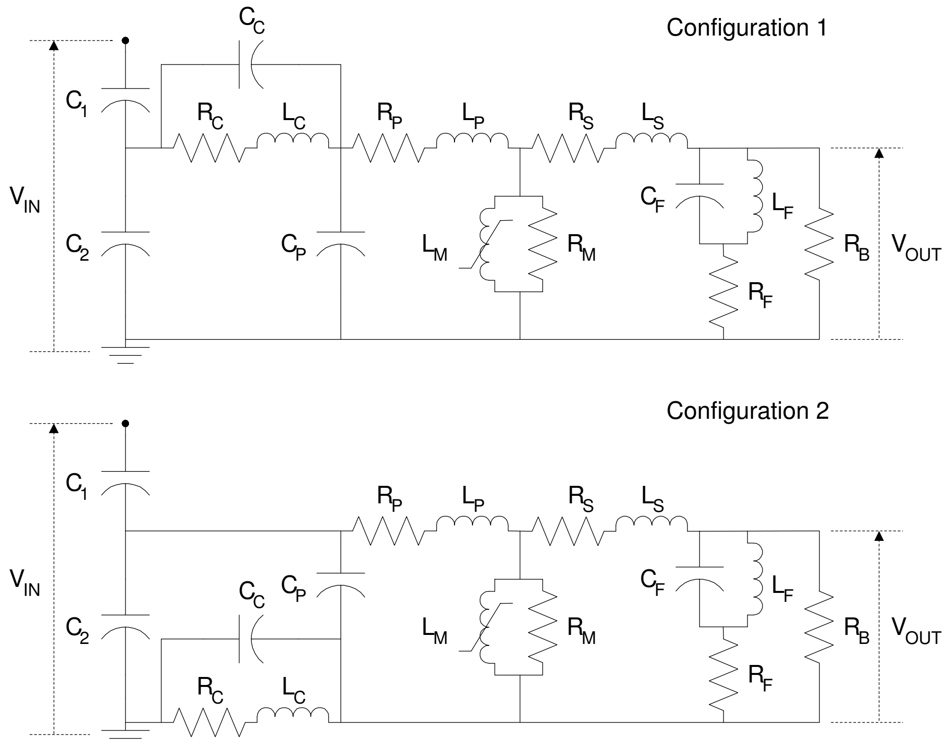

Fig. 35. Configurations of CCVT models

Model A represent a line overcurrent protection relay. The model offers the following features:

- Three-phase directional instantaneous overcurrent relaying, if used as a primary protection
- Three-phase time overcurrent relaying, if used as a backup protection

The elements and flowchart of model A are shown in Fig. 36. Elements of the IED model A are:

- Measuring algorithm performs extraction of current and voltage phasor from the signals supplied by instrument transformers. Extraction is performed by

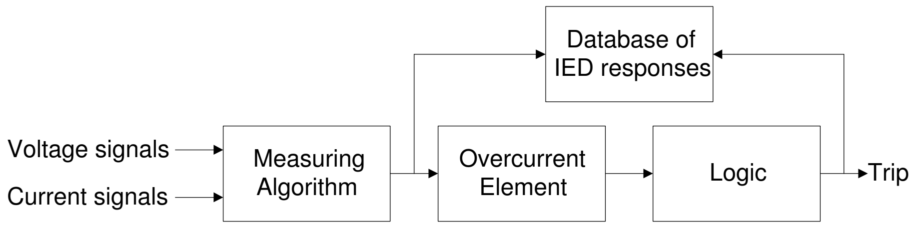

Fig. 36. Elements and the flowchart of the IED model A

Fourier algorithm. The phasor values are multiplexed together and sent to overcurrent element.

- Overcurrent element consists of three sub-elements, each providing protection by a certain operating principle. The sub-elements are:

  1. Time overcurrent protection. This protection provides fast operation time for high fault currents, and slow operation when light currents are detected. This results in inverse time characteristic.

  2. Ground time overcurrent protection. This protection operates when a fault involving ground is detected. It uses the same type of characteristics as the time overcurrent protection.

  3. Directional protection. This protection is designed to operate for faults in a certain direction. This protection element uses direction of the flow of the current or power to determine whether a fault is in the direction of protected line.

- Logic element applies logic functions (AND,OR) on the assertion signals produced by the protection element and operates the circuit breakers only when a fault current is sufficiently high and when the fault is detected in the direction of interest. Otherwise, logic element restraints the relay from asserting the trip signal.

Output signals of IED model A are available for capturing. They are recorded to database of IED responses, together with trip signals. Settings for the IED model A are:

- Nominal current on input of IED model is I_n=5 A.
- Pickup current is set to twice the nominal value: I_{pickup}=10 A.
- Extra inverse time-current characteristic was used. This characteristic is defined as [32]:

$$t_{operate} = \frac{13.5 \cdot k}{I_n - 1} \tag{5.1}$$

  Time-parameter k was chosen as: k=0.02. This characteristic allows for efficient distinction between near-end and far-end faults on the protected line Sky-STP, because of the parameters of the transmission line (length and impedance). More on the selected inverse-time characteristic can be found in reference [32]. The plot of characteristic is shown in Fig. 37.

IED model B represents a transmission line distance (impedance) protection relay. Protection features implemented in the model are [29]:

- Three separate MHO forward sensing zones for multi-phase faults
- Three separate quadrilateral forward sensing zones for phase to ground faults
- One MHO reverse sensing zone for multi-phase faults
- One quadrilateral reverse sensing zone for phase to ground faults
- Six separate MHO starters, one for each fault-measured loop

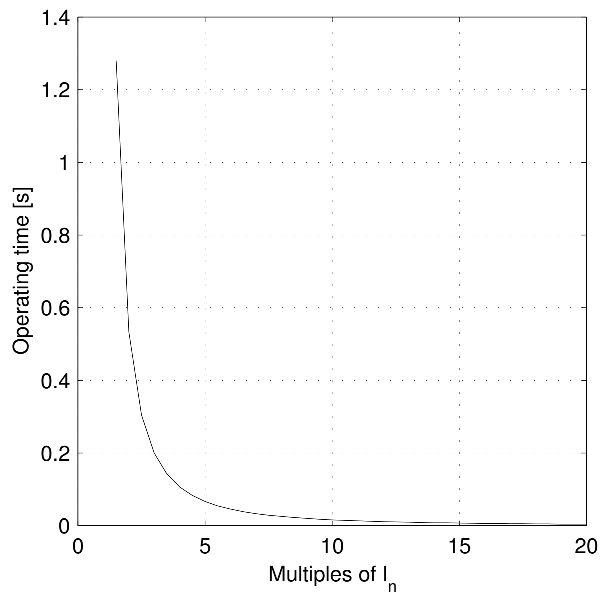

Fig. 37. Inverse time-overcurrent characteristic of the IED model A

- Undervoltage element

The elements and flowchart of model B are shown in Fig. 38. Elements of the IED model B are:

- Measuring algorithm calculates fault impedance using differential equation algorithm. Fault impedance is calculated according to fault expressions for 6 basic types of faults (AG, BG, CG, ABC, BC, CA). The calculation is performed using combinations of input currents and voltages. Fault impedance is calculated for every of the six types of faults and sent to the fault identification element.

- Fault calculation element determines whether calculated impedance represents a fault within zones of protection. The check is performed for every zone and for every fault type. The output of the element is a signal indicating whether there is a fault. Output signals for each of the zones are multiplexed and sent

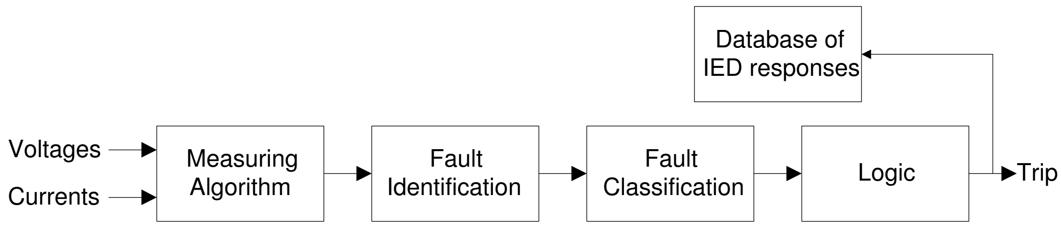

Fig. 38. Elements and the flowchart of the IED model B

to the fault classification element.

- Fault classification element determines the type of detected fault. The output of this element is not necessary for the assertion of trip signal. However, it provides valuable information for the protection engineers.

- Logic element performs logic operations to derive a correct trip signal. Logic functions such as AND, OR are used to trip in the case of a fault or trip restrain for a fault out of the operational zones.

IED model B does not allow for capturing of the output signals of the measuring algorithm. Only the trip signals can be recorded. Settings for the IED model B are:

- Two zones of protection are set. First (primary) zone of protection covers 80% of Sky-STP transmission line ($Z_{Sky-STP} = 95.4\angle 83.81°\Omega$). Intentional trip time-delay for faults detected in this zones is set to 0 ms. Second (backup) zone covers remainder (80% through 100%) of the Sky-STP transmission line. Time-delay for trip for the faults in this zones is set to 20 power system cycles (333 ms).

- Operating characteristics are selected as mho zones. The operating characteristics, as well as the protected line itself, are shown in Fig. 39.

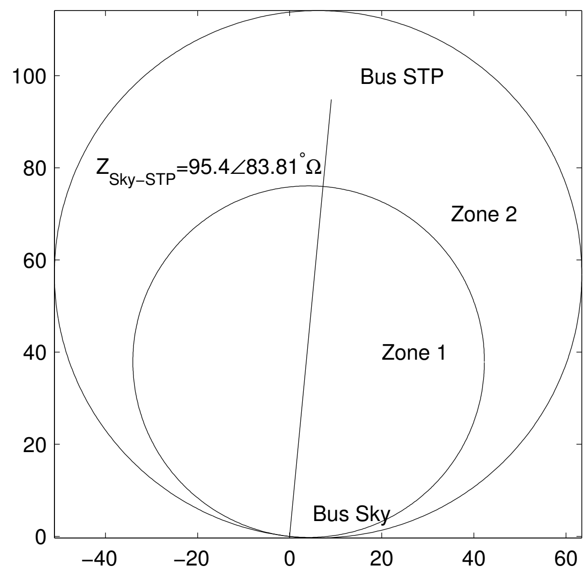

Fig. 39. Coverage of MHO zones of the IED model B

Connection of IED models to instrument transformer models and power network model are shown in Fig. 40.

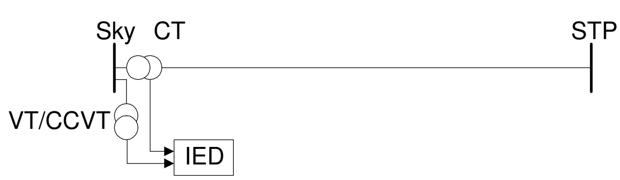

Fig. 40. Connection of IED and instrument transformer models

D. Simulation Scenarios

Events are organized according to simulation scenarios. The scenarios definition consists of:

1. Timeline of events

2. Features of events

Timeline defines time points when each of the events starts and when it finishes. Event is usually modelled by a sequence of switching of power network circuit breakers. Switchings allow for a modification of network topology, thus simulating faults and disturbances. The events are characterized by their features. Examples of features are: location of the event along the transmission line, associated resistances (such as ground or line-to-line resistances), point-on-wave of fault inception and so on.

In this thesis, two scenarios were defined, for two models of IEDs. The events were selected to emulate situations when the influence of instrument transformers can be critical.

Different scenarios were defined for IED models A and B, as shown in Tables VII and VIII. In the case of IED model A, faults were simulated both in forward and backward zone of protection. IED model is expected to operate for faults in the forward zone of protection, while it is expected to restrain from operating (issuing a trip signal) for faults in the backward zone of protection. In the case of IED model B, faults were simulated in zones 1 and 2. Fault locations were chosen to test IED response of both primary and backup zone of protection.

Three types of faults are simulated: phase-to-ground (AG) and phase-to-phase (BC) faults, as well as their combination (ABCG). The model should be transparent to different types of faults (considering selectivity and operational time). Every fault

Table VII. Simulation scenario, IED model A

Feature	Parameters
Fault type	AG, BC, ABCG
Fault location [%]	-10, 10, 70, 90
Resistance [Ω]	0, 5
Point-on-wave [deg]	0, 45, 90, 135, 180, 225, 270, 315

type is simulated at four locations along the (protected) Sky-STP line. In the case of testing IED model A, locations are: -10 %, 10 %, 70 %, 90 %. First location, -10 % means that faults are simulated in the backward direction, on the line Sky-Spruce (starting from bus Sky). When testing IED model B, locations are: 70 %, 75 %, 85 % and 90 %. Faults at the first two locations should be detected (by IED model B) as belonging to the first zone, while faults at second two locations should be detected as belonging to second zone. Locations at 75 % and 85 % (of the line length) are close (in relaying terms) to the 80 % zone boundary. These locations were chosen to check whether IED model may underreach or overreach. Every fault is simulated using two fault-resistances: 0Ω and 5Ω. In the case of phase-to-ground faults, the resistance is the phase-to-grounding resistance, while in the case of phase-to-phase faults, the resistance is the phase-to-phase resistance. The value of 5Ω was chosen to emulate fault resistance that can be found in realistic situations. Finally, every fault

Table VIII. Simulation scenario, IED model B

Feature	Parameters
Fault type	AG, BC, ABCG
Fault location [%]	70, 75, 85, 90
Resistance [Ω]	0, 5
Point-on-wave [deg]	0, 45, 90, 135, 180, 225, 270, 315

is simulated starting at 8 different fault inception moments (point-on-wave), covering range of one 60 Hz cycle in 8 equal, consecutive time-steps. Total number of cases generated for each of IED models is: $3 \cdot 4 \cdot 2 \cdot 8 = 192$.

E. Benefits and Limitations of the Simulation Approach

Simulation approach has distinctive benefits, as well as limitations, when compared to different approaches, such as hardware testing. When deciding upon the use of the simulation approach, both the limitations and benefits should be carefully considered.

Benefits of the simulation approach are:

- In the evaluation stages, problematic components of instrument transformers can be identified using simulation approach. This is valid under assumption that models of instrument transformers and protective relays are available for evaluation.
- Simulation approach is a great tool for educational purposes. It provides a novel insight into evaluation of influence of instrument transformers on internal components of IEDs. This insight creates much better understanding of interaction between instrument transformers and power system protection system.

Limitations of the simulation approach are:

- Evaluation of existing instrument transformers and IEDs is limited by the availability of models of devices. At present, there is only a small number of commercial protective relay and instrument transformer models (in the available literature). In other cases, models may exist but may not be readily available to the user.

- Most of the commercial protective relays do not provide access to output signals of the measurement unit. Some commercial relays (e.g. SEL-321) provide recordings of some internal measurements. The mentioned recording can be used to derive some of the performance indices (allowing for at least partial use of simulation approach).

F. Conclusion

This chapter described simulation approach to evaluation of influence of instrument transformers. First, details about the approach, such as types of data and procedures to be used, were discussed. The role of models was also addressed. Next, models of power network, instrument transformers and IEDs were described. The reasons for choice of models was explained. Elements and structure for each IED model were also presented. Settings for IED models were defined. Afterwards, simulation scenarios were defined. Event features of scenarios were selected to exacerbate possible critical influence of instrument transformer models on IED models.

Conclusion of the chapter is that by proper choice of models, effective and meaningful results can be obtained through simulation. An advantage of simulation approach over field collected data was pointed out: amount of data collected from field recording can be insufficient for proper evaluation of influence of instrument transformers. Therefore, simulation approach is a suitable mean for implementing the evaluation methodology.

Material presented in this chapter is a theoretical background for the next chapter. Next chapter describes software implementation of simulation approach: simulation environment.

CHAPTER VI

SOFTWARE IMPLEMENTATION

A. Introduction

Simulation environment was developed to support the evaluation methodology. The implementation consists of several software modules that can be used either individually, or as combined package. Simulation environment is expandable. Existing software modules can be modified (adjusted) or new modules can be added to the package, according to needs and objectives of the user.

Structure of input and output (I/O) data is shown in Fig. 41. As can be seen, the environment allows the user to evaluate different combinations of various models of power networks, IEDs and instrument transformers. The evaluation of the same models can be done under multiple different event scenarios. Output data consists of numerical values of performance indices (see Chapter IV).

Main features of the environment are *automation* of the test procedure, *compre-*

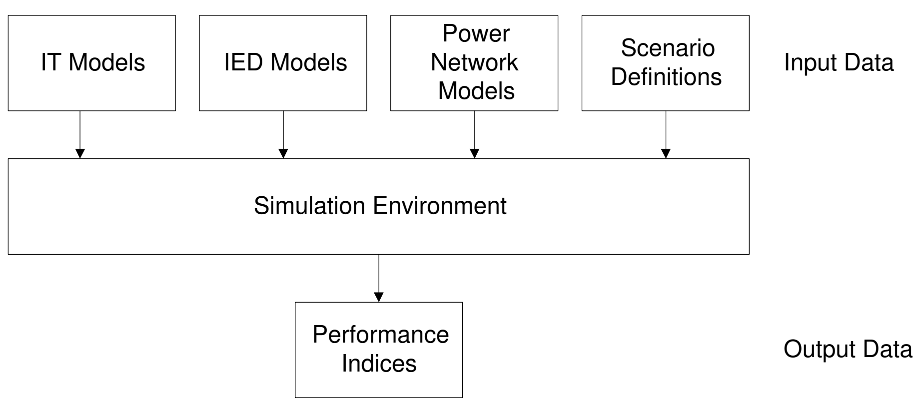

Fig. 41. Structure of the I/O data

hensiveness of the results and *flexibility* of the use. Automation means that testing is performed with a minimal user interaction (without any loss of accessibility or modifiability of relevant simulation parameters). The comprehensiveness means a sufficient number of test cases is always covered, while each case presents protection system conditions with a sufficient number of parameters. Flexibility means: 1) different instrument transformer and IED models can be integrated into testing, allowing the user to test and compare influence of various instrument transformer versions and designs, 2) results can be generated in the form of graphs and tables that can be directly imported into various text processors, allowing the user to quickly and efficiently analyze final results.

This chapter describes elements, structure and software implementation of the simulation environment. Special attention is given to explaining I/O structures and flowcharts of various elements. The reason for doing so is to give information to the user who wishes to modify or expand the environment, or wishes to use data generated by the environment in additional studies. User interface is also discussed.

B. Structure of the Simulation Environment

Main functional elements and flowchart of the environment are shown in Fig. 42. There are three main elements:

1. Exposure generator

2. Exposure replayer

3. Statistical analyzer

Output of the environment are tables containing numerical values of performance indices (see Chapters IV and V). In the process of derivation of mentioned indices,

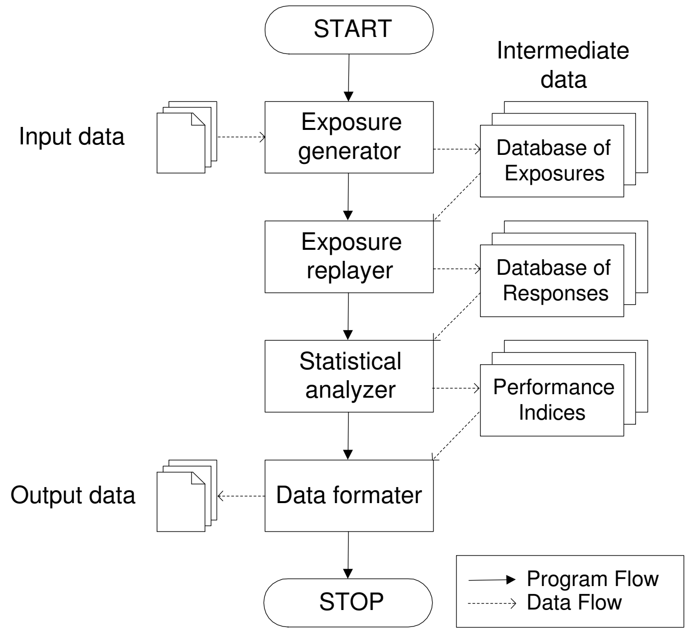

Fig. 42. Flowchart of the simulation environment

environment creates three databases of intermediate results. The databases are:

1. Database of exposures
2. Database of model responses
3. Database of performance indices

The following section describes options for implementation of the software environment and databases.

C. Options for Software Implementation

There are many possible options for software platforms that can be used to implement simulation environment. The following software packages have been used to develop the environment:

- Alternative Transient Program (ATP) [23]. This program is a version of Electromagnetic Transient Program (EMTP). Purpose of ATP package is simulation of transient waveforms associated with electromagnetic phenomena in power networks. Program also has the option of frequency analysis. ATP development was continuous over the last 20 years. Contributors in development are international, while the coordinator is the Canadian/American ATP Users Group (available online: www.emtp.org).

  Input of ATP are text files, called scripts. Scripts consist of a list of power network elements and their connections. Together, elements and connections define a model of a network. Basic operation of ATP is calculation of variables of interest (current and voltages), as functions of time. Variables of interest are defined by the user. Calculation is based on solving differential equations that describe behavior of system components in time domain. Trapezoidal rule of integration is used for solving. There are two ways of determining initial conditions: 1) initial steady-state (phasor) solution of the system model, 2) initial values specified by the user (for some components).

  Extensive library of power system component models is available in the current version of ATP. Models include: rotating machines, transformers, surge arresters, transmission lines, cables, etc. By combining mentioned components, complex networks can be built. Additional feature of the program allows for analysis of control systems, power electronics equipment and components with nonlinear characteristics, such as arcs, corona and saturable electromagnetic core. When simulating events, both symmetric and asymmetric disturbances are allowed.

- Matlab [33]. The name Matlab stands for Matrix Laboratory. Matlab is a high-

Table IX. Implementation of the software environment

Package	Usage
ATP	Implementation of power network and instrument transformer models Generation of exposure waveforms
Matlab	Replaying of exposure waveforms Statistical analysis of IED model responses Creation of output data tables
Simulink	Implementation of IED models Generation of IED response signals

performance language for technical computing. It represents the state-of-the-art in software for matrix computation. One of the main parts of the program is Matlab language. This language is a high-level matrix/array language, with control flow statements, functions, data structures, input/output and object-oriented programming features. Such a structure allows for creating large and complex application programs using relatively simple instructions.

- Simulink [34]. Simulink is Matlab's companion program. Its purpose is simulating nonlinear dynamic system models. Types of systems that can be modelled using Simulink include linear, nonlinear, continuous-time, discrete-time, multi-variable and multi-rate. Main feature of the program is attractive, easy-to-use graphical user interface (GUI). This interface allows for building of models by simply placing system components on the work sheet and specifying connections between them. In order to simulate power network systems, Power Blockset can be used [35]. This blockset is an additional library of system components that model power network elements. Power blockset presents a specialized application of Simulink.

Table IX gives an overview of implementation options for the software environment.

Table X. Simulation environment installation files

Directory	Content (files)
scenario_scripts	insert_fault_distributed.m, insert_fault_lumped.m, branch_distributed.m, insert_parameters.m, branch_lumped.m, insert_vt.m, cases.m, parameters.m, connection.m, resistor.m, cp.m, s_fmt.m, ct.m, s_fmt_cardinal.m, ct_model.m, scenario.m, dl.m, setup.m, exec.m, exposures.m, swtch.m, extract_steady_state.m, uniform_names.m, fault.m, vt.m, init.m, vt_model.m, insert_ct.m, insert_fault.m
overcurrent_scripts	dec_data.m, meas_data.m, oc_data.m, overcurrent.m, get_signals.m, oc_average.m, oc_test.m
distance_scripts	d_average.m, d_dec_data.m, distance.m, d_data.m, d_test.m
general_scripts	flip_slashes.m, get_list.m, create_table.m, remove_underscore.m
models	StpPlain10kHz5sec.atp, HYST.pch, HYST_2.pch, ml.m, fl.m

D. Simulation Environment Setup

Simulation environment consists of Matlab and ATP script files. The files are organized in five directories. The contents of the directories are shown in Table X. The mentioned files are delivered as a single ZIP file "simenv.zip". This ZIP file is an archive, containing the files and directory structure shown in Table X. Once decompressed (unpacked), the simulation environment is ready for use. The directory where the simulation environment software files are stored is designated as "root" directory (use of this directory is discussed in more detail in Section E). The location of "root" directory can be specified through simulation environment initialization (described in more detail in Section E). In order to use the simulation environment, the following software packages should be installed on the computer:

1. Matlab (recommended version 5.3 [33], other versions not tested for compatibility)

2. Simulink (recommended version 5.3 [34], other versions not tested for compatibility)

3. ATP (recommended version compiled by Watcom Fortran [23], other versions not tested for compatibility)

E. Initialization of the Simulation Environment

Before running the simulation environment, it is necessary to perform initialization. This is done by invoking script "init.m". This script defines necessary global variables (variables that are accessible from every other script). Some important global variables are:

- **root**: this variable defines the location (path) to the simulation environment files. This location can be freely adjusted by the user.
- **models**: this variable defines the location (path) to models of power network

Another important aspect of initialization is creation of database structure. Once the script "init.m" is finished with execution, all the necessary directories and subdirectories are created (within the root directory) (databases are discussed in more detail in text to follow).

F. Exposure Generator

The most complex module of the environment is the exposure generator. As the name implies, objective of this module is building a database of exposures.

1. I/O Data Structure

Input of the module consists of:

1. Scenario definition
2. Instrument transformer models

```
fault_bus1='Sky';
fault_bus2='STP';
fault_type=[1,2,5];
fault_location=[10,70,90];
fault_resistance=[1e-6,10];
fault_time=[0,1,2,3,4,5,6,7,8]*0.01667/8;
```

Fig. 43. Definition of a scenario

3. Power network models

Scenario definition was discussed in Chapter V. Scenario for the simulation environment can be defined within script “exposures.m”. The definition simply lists event features. As an example, definition of a scenario for evaluation of CCVT models (as discussed in Chapter V) is shown in Fig. 43.

The input data in a form of event features should be supplemented with the data about location of instrument transformers and their connections to the power network model. This supplemental information is also specified within script “exposures.m”. An example is shown in Fig. 44.

The above-given input data specifies that the current transformer is connected at the Sky bus, of Sky-STP line, as stated in the variables **ct_node1** and **ct_node2**. CT scale-down ratio is defined as 900:5, using variable **ct_ratio**. Even though specific

```
ct_node1='Sky';
ct_node2='STP';
ct_ratio=900:5;
ct_burden=low_burden;
ct_model=1;
vt_node='Sky';
vt_ratio=345e3/112;
vt_burden=inductive_burden;
ct_model=2;
```

Fig. 44. Specifying instrument transformer connections with power network

current transformer models used with the environment may have pre-set scale-down ratio, user is still left with the freedom to manually set this ratio. The reason for this is to allow small modifications to the ratio, usually in the limits of ±5% (e.g. current transformer model with the ratio of 900:5 ca be used in simulations as having the ration of $(1.05 \cdot 900 : 5)$. The same kind of specification are made for the CCVT, using variables **vt_node** and **vt_ratio**.

Output data of exposure generators are the files containing exposure waveforms (3 current and 3 voltage waveforms, corresponding to three phases). Waveforms are stored in the form of Matlab matrix files. Matrix and vector variables which comprise exposure file are:

1. Time vector **t**. Contains time scale produced by ATP.

2. Primary voltage signal vectors **vVtnodea**, **vVtnodeb**, **vVtnodec**. Mentioned three vectors contain primary voltages, corresponding to three phases. **Vtnode** is the name of the node where voltage transformer (or CCVT) is connected.

3. Secondary voltage signal vectors **vVta**, **vVtb**, **vVtc**. These three vectors contain signals from the output of voltage transformer/CCVT models.

4. Primary current signal vectors **iTerraCtsa**, **iTerraCtsb**, **iTerraCtsc**. Mentioned three vectors contain primary current signals, from the transmission line where current transformer is connected.

5. Secondary current signal vectors **iCtnodeaCtpa**, **iCtnodebCtpb**, **iCtnodecCtpc**. These vectors, corresponding to three three phases, are obtained from secondaries of current transformer model. **Ctnode** is the name of the node (bus) where current transformer model is connected.

6. Steady-state current phasor matrix **i_ss**. These phasors, one for each phase, correspond to currents in the transmission line (under investigation) during steady-state faulted condition (after transient signals die-out). First row of the matrix contains phasor magnitudes, while second row contains phasor angles.

7. Steady-state voltage phasor matrix **v_ss**. Explanation is the same as for matrix variable **i_ss**.

8. Moment of the event start **t_start** (scalar). This is scalar value that denotes (in [s]) when the event starts.

9. Additional information **fault_data**, **ct_data**, **vt_data**. This data is simply copied content of scenario definition and instrument transformer connection specifications (see Figs. 43 and 44). The reason for including these fields in the structure is to enable efficient sorting of exposure files, when storing them into the database.

The above vectors and matrices are nested within an object structure, denoted **signals**. Therefore, each of the vectors or matrices can be accessed by putting the object structure name (followed by a period) in form of the vector or matrix name, e.g. **signals.iTerraCtsa**. An example of an exposure structure is shown in Fig. 45.

Exposure files are stored (organized) in the form of database. The structure of the exposure database, created for scenarios defined in Chapter V, is shown in Table XI. According to the table, root directory contains every one of the main directories. In turn, each main directory contains all the subdirectories. Prefixes "oc_" and "d_" denote IED model A ("oc" is short for overcurrent) and IED model B ("d" is short for distance), respectively. All the exposure files, once generated, are stored in directory called "exposures", corresponding to IED and instrument transformer model. Utility script “cp.m” can be invoked afterwards to copy the exposure files from the mentioned directory “exposures” into appropriate subdirectories, that classify the exposure files according to the fault type (e.g. “d_exposures_abcg”).

Once an exposure is generated, it is stored into appropriate directory location by the exposure generator. Complementary to database structure is the exposure file naming system. Exposure files are named according to event features (event which, through simulation, produced the exposure). Features that are used for file naming are:

1. Nodes (bus) names of the line, where event takes place
2. Type of fault (capital letters)
3. Grounding resistance (denoted by letter ’r’)

```
signals =
              t: [1835x1 double]
          vSkya: [1835x1 double]
          vSkyb: [1835x1 double]
          vSkyc: [1835x1 double]
           vVta: [1835x1 double]
           vVtb: [1835x1 double]
           vVtc: [1835x1 double]
    iTerraCtsa: [1835x1 double]
    iTerraCtsb: [1835x1 double]
    iTerraCtsc: [1835x1 double]
     iSkyaCtpa: [1835x1 double]
     iSkybCtpb: [1835x1 double]
     iSkycCtpc: [1835x1 double]
           i_ss: [2x3 double]
           v_ss: [2x3 double]
        t_start: 0.0646
     fault_data: [1x1 struct]
        ct_data: [1x1 struct]
        vt_data: [1x1 struct]
```

Fig. 45. Structure of an exposure

Table XI. Structure of the exposures database

Root Directory	**Main Directories**	**Subdirectories**
results	ct_ref ct_1 ct_2 ct_3 ct_4 ccvt_1 ccvt_2 ccvt_3 ccvt_4	exposures oc_exposures_abcg oc_exposures_ag__ oc_exposures_bc__ d_exposures_abcg d_exposures_ag__ d_exposures_bc__

4. Location of the fault along the line (denoted by letter 'l')

5. Index number of time-point of the event (denoted by letter 't')

The features are included in the file name in the order as given above. All files carry extension 'mat', which is standard extension for Matlab matrix files. An example of the exposure file name is "FAULT_Sky_Spr_AG___r5__l10_t4.mat"

2. Flowchart

Flowchart of the exposure generator is shown in Fig. 46. Generation of transient waveforms (exposures), corresponding to scenario events, is carried out by invoking ATP software. Exposure generator creates a script file based on models of power network, instrument transformer models and scenario definition (input data). Flowchart of the algorithm that performs the creation of the script is shown in Fig. 46(b). The algorithm reads line-by-line the text file containing description of the network model. Every line is analyzed until the line containing information about protected transmission line is found. Once it is found, it is divided into two lines, by inserting a new bus in the original line. New bus is a point on the line where events can be simulated

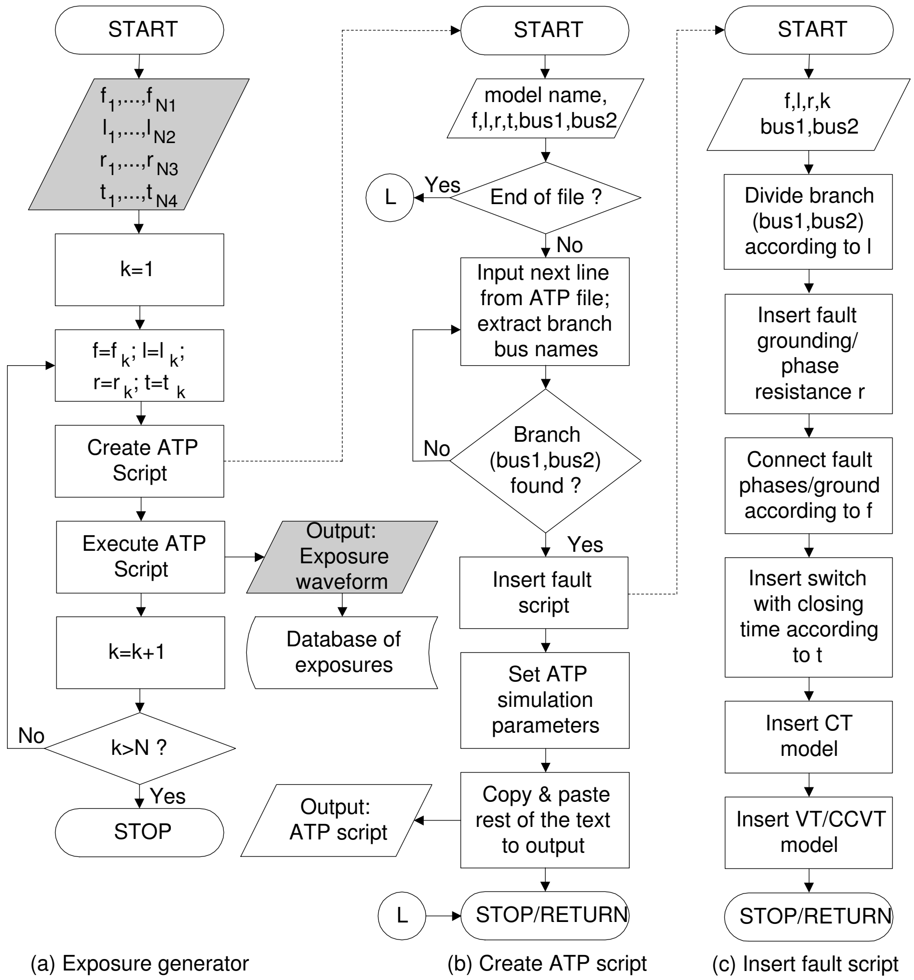

Fig. 46. Flowchart of the exposure generator

(e.g. faults). Ratio of impedances of newly formed lines is chosen to simulate location of the event, along the line. Total impedance of both (sub)lines is equal to the impedance of the original line. This process is illustrated in Fig. 47.

The figure illustrates division of the protected line Sky-STP. Figure shows only one phase of the three-phase line (other phases involve same circuitry). New bus, named 'Sky1' is inserted. The impedance of the segment Sky-Sky1 is 25% of the original Sky-STP line. This way, the location of the simulated event is fixed at 25%

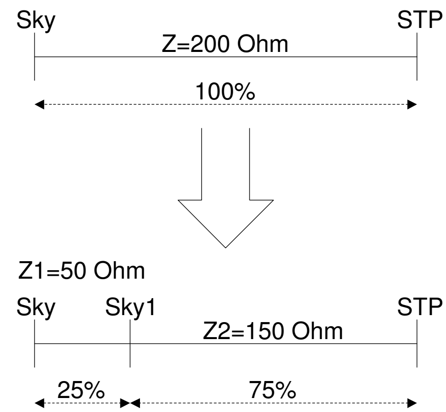

Fig. 47. Division of a transmission line (branch)

of the line length. The actual division of the line is performed by an algorithm, shown in Fig. 46(c). This algorithm generates text lines, that are inserted into the original ATP script. At this point, instrument transformer models (current transformer and voltage transformer/CCVT) are also inserted, in the form of text lines. The text lines define new buses and connections, as shown in Fig. 48. In the figure, labels (names) in italic (e.g. *Sky*,*STP*,etc.) denote labels of the nodes, while normal-type labels denote respective component value (e.g. C_1 is the value of capacitance). An example of ATP script generated by the exposure generator can be found in Appendix A.

After the circuit shown in Fig. 48 is inserted, a time-point for closing the switch is specified (t_{open} in the figure). Closing of the switch simulates a fault. By placing the switch at suitable locations, both phase-to-ground and phase-to-phase faults can be simulated. Former faults are simulated by placing switch between two phases (lines). Ground faults involve placement of switch between phase (line) and ground, as illustrated in Fig. 48.

The final script file is created when both the fault and instrument transformer

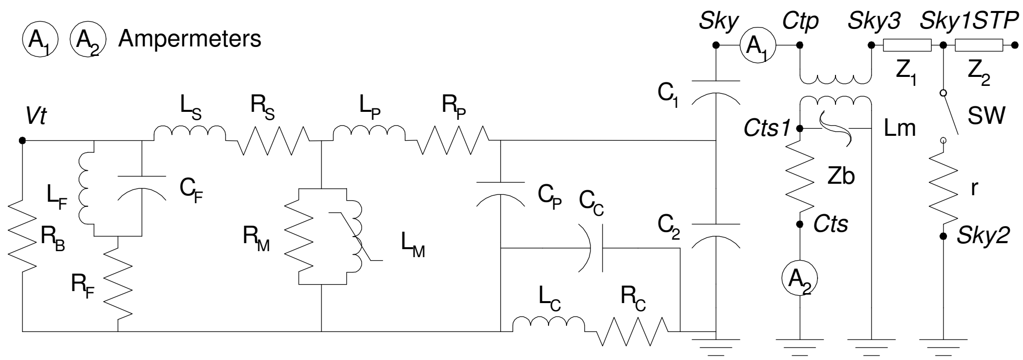

Fig. 48. Insertion of the fault and instrument transformer connections

circuits have been inserted. This script is processed once more, to insert simulation parameters, such as duration of simulation (in [s]), time-step (in [s]), power system frequency (in [Hz]), and similar (more on these parameters can be found in reference [23]). The final script is then sent to ATP for execution. During the execution of ATP script, flow control is surrendered to ATP. When ATP is finished with generating the transient waveform, flow control is returned to the exposure generator. Next step is to check whether all the scenario events have been executed ($k > N$, where k is the index number of currently simulated event, while N is total number of events in scenario). Exposure generator is terminated when a scenario has been completed. Once the database of exposures has been built, exposures replayer can be used to expose IED models to captured waveforms. Exposure replayer is described in the next section.

G. Exposure Replayer

Objective of the exposure replayer module is exposing IED models to waveforms corresponding to power system events. Replayer module obtains mentioned waveforms from the database of exposures, generated by exposure generator. Other sources can also be used, such as custom-built database of field-recorded data.

1. I/O Data Structure

Input of the module consists of:

1. Pointer to database of exposures

2. Pointer to IED models

First pointer is variable **root** (global variable), which value specifies root directory location of the exposure database (see Table XI). Second pointer is the file name of the Simulink model of IED (this point will be discussed in more detail in the text to follow).

Output of exposure replayer are files containing IED model response signals. As before, files are stored as Matlab matrix files, with standard extension "mat". In the case of IED model A, mentioned signals are recorded at two points:

1. Output of measuring element

2. Output of decision making element

In the case of IED model B, signals are recorded only at output of decision making element.

File naming system used in the exposure replayer is similar as in the exposure generator. The only difference is in the file name prefix. Measuring element output is stored in the file named starting with "OC_M" ("M" is short for measuring), while decision making element output is stored in files starting with "OC_D" and "D_D" ("D" is short for decision making).

Measuring file contains two object structures, called **i** and **v**. Both structure contains the same variables. In the case of structure **i** mentioned variables contain signals from current-measurement element, while in the case of **v**, the signals are from voltage-measurement element. The variables are:

1. Steady-state phasor matrix **ss**. The meaning of this variable is the same as in the case of exposure generator (see previous section).

2. Measured phasor magnitude and phase vectors **a_amp**, **a_ph**, **b_amp**, **b_ph**, **c_amp**, **c_ph**. These vectors contains signals measured by the Fourier algorithm measuring element.

3. Original exposure waveform vectors **a**, **b**, **c**. Vectors containing copies of original waveforms (that are sent to the input of measuring element), corresponding to three phases, are included for use by statistical analyzer, which will be discussed in the next section.

4. Time vector **t** and moment of the event start **t_start** (scalar). Meaning is similar to the exposure generator (see previous section). There is difference, however: the time scale, contained in vector **t** is generated by Simulink, which may be (and usually is) different than the one generated by ATP. ATP generates time scale with equally spaced time-points, while Simulink, depending on the chosen solving method, may produce time scale where time-steps are not equal.

Decision making file contains two vector and one scalar variable. The variables are:

1. Time vector **t** and moment of the event start **t_start** (scalar). Meaning is the same as in the case of the measuring file.

2. Trip signal vector **trip**. This vectors contains trip signal derived by decision making element.

Mentioned measuring and decision making files are stored (organized) in the form of database. The structure of the response database, created for scenarios defined in Chapter V, is shown in Table XII. This database has the same structure as the database of exposures (see Table XI). The content of the response database is complementary to content of exposure database. Together, the two databases form one, general database. This database can also be used outside the simulation environment.

2. Flow Chart

Flowchart of the exposure generator is shown in Fig. 49(a). Replayer performs a loop, in which exposures are sequentially read from the database, and replayed. The loop is performed until the database has been exhausted ($k > N$, where k is the index number of currently replayed exposure, while N is total number of exposures in database). Actions performed to replay an exposure are:

1. Set variables **i_in** and **v_in** to contain exposure. The content of these variables is sent directly to IED model using Simulink. The Matlab code that performs this is shown in Fig. 50. In the code, variable **s** contains exposure (see Fig. 45), while variable **ref_flag** determines what instrument transformer is being evaluated (referent instrument transformer, current transformer or voltage transformer/CCVT). Variables **i_in** and **v_in** are a communication channel between simulation environment and Simulink. This communication is shown in Fig. 51. Different IED models can be incorporated into simulation environment by observing structure of variables **i_in**, **v_in**.

2. Execute Simulink model file. By starting the simulation, flow control is temporarily transferred to Simulink. The flow control is returned to exposure replayer once the exposure has been replayed, and necessary IED response data has been recorded. The execution of IED model is done using command **sim('systemtotal',t_max)**. The sequence "systemtotal.mdl" is the file name of overcurrent protection IED model implemented in Simulink (hence the extension "mdl"). It can be replaced by any other model of an IED, provided that the model complies with simulation environment as shown in Fig. 51.

Table XII. Structure of the database of IED responses

Root Directory	**Main Directories**	**Subdirectories**
results	ct_ref	oc_abcg
	ct_1	oc_ag__
	ct_2	oc_bc__
	ct_3	d_abcg
	ct_4	d_ag__
	ccvt_1	d_bc__
	ccvt_2	
	ccvt_3	
	ccvt_4	

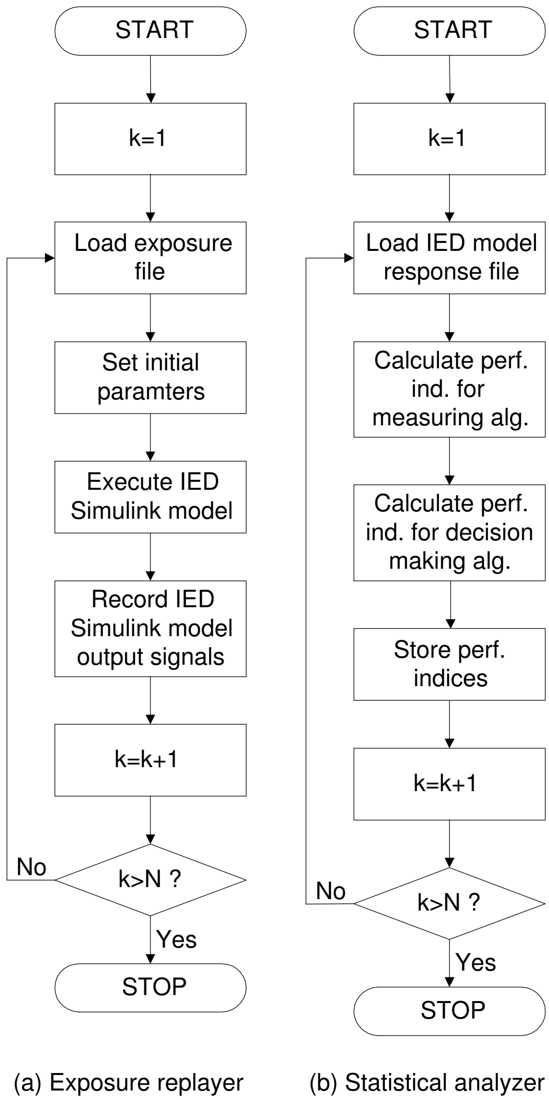

Fig. 49. Flowchart of the exposure replayer and the statistical analyzer

```
s=get_signals(var);
switch(ref_flag);
case 1
   % referent testing:
   % primary current signals referred to secondary
   i_in.signals.values=s(1:3,:)'/ct_ratio;
   % primary voltage signals
   v_in.signals.values=s(7:9,:)';
case 2
   % ct testing:
   % secondary current signals
   i_in.signals.values=s(4:6,:)';
   % primary voltage signals
   v_in.signals.values=s(7:9,:)';
case 3
   % vt testing:
   % primary current signals (referred to secondary)
   i_in.signals.values=s(1:3,:)'/ct_ratio;
   % secondary voltage signals referred to primary
   v_in.signals.values=s(10:12,:)'*vt_ratio;
end;
i_in.time=s(13,:)';
v_in.time=s(13,:)';
```

Fig. 50. Matlab code for setting input variables

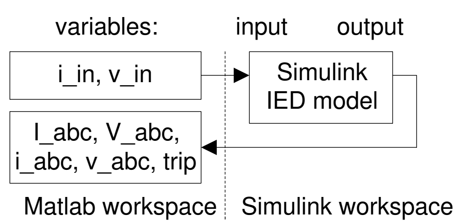

Fig. 51. Communication between the simulation environment and Simulink

H. Statistical Analyzer

Objective of the statistical analyzer is derivation of numerical values of performance indices, defined in Chapter IV. The calculation is carried out as described in Chapter IV.

1. I/O Data Structure

Input of the statistical analyzer is a pointer to top of the database of responses (path to root directory). This pointer is specified using variable **root** (global variable).

Output of statistical analyzer are files, containing performance indices. Files are stored as Matlab matrix files, carrying extension "mat". In case of IED model A, the indices are calculated for both measuring and decision making elements, while in case of model B, indices are calculated only for decision making element.

File naming convention used in the statistical analyzer is simple: file name prefix for IED model A is "OCDATA_", and for model B the prefix is "DDATA_". The prefix is followed by the instrument transformer model, which was used in simulations for derivation of particular indices (stored in the file). Prefix is followed by the name of instrument transformer model. An example of a file containing performance indices is "OCDATA_ct_1.mat". Mentioned files are stored according to the structure of the response database, shown in Table XII. One file, containing performance indices, is stored in each of subdirectories.

Performance indices file contains two structures: **m** and **d**. The first one contains performance indices for measuring element, while the second structure contains indices for decision making element. First structure is present only in the case of IED model A indices.

Structure **m** has two sub-structures: **i** and **v**. First sub-structure contains indices for current measuring element, while second sub-structure contains indices for voltage measuring element. The variables contained in sub-structures are:

1. Gain for the DC component **dc_gain_a**, **dc_gain_b**, **dc_gain_c**.

2. Aggregated index F **F_a**, **F_b**, **F_c**.

3. Settling time **s_a**, **s_b**, **s_c**.

4. Overshoot **o_a**, **o_b**, **o_c**.

5. Normalized error index, **e_a**, **e_b**, **e_c**.

Structure **d** has two scalar variables:

1. Time-point of the start of event scalar **t_start**.

2. Time-point of issuing a trip signal **t_trip**. In the case of IED model B this variable is not scalar, but a two-element vector, where first element denotes trip time for zone 1, and second element denotes trip time for zone 2.

Performance indices file contains a sequence of sets of indices. Sets from one file correspond to a subdirectory of a database of IED response. Subdirectories within the structure of this database is where performance indices files are stored.

2. Data Formatter

Additional utility scripts, data formatters called "oc_average" and "d_average", can be used for finding *average* values of performance indices. Average values are found by analyzing every file of performance indices and simply calculating the mean value of all the indices store in that particular files. Mentioned utility modules also have the ability of generating output data in form of tables. Tables can exported as:

- Matlab matrix, in the form of "mat" matrix file
- Plain ASCII text
- LaTeX format tables

3. Flowchart

Flowchart of the statistical analyzer is shown in Fig. 49(b). Similar as replayer, statistical analyzer performs a loop, in which IED responses are sequentially read from the database and analyzed. Analysis is the actual calculation of performance indices, in accordance with definitions in Chapter IV. The loop is performed until the response database has been exhausted ($k > N$, where k is the index number of currently analyzed response, while N is total number of responses in database).

I. User Interface

User interface is in the form of Command Line Interpreter (CLI). Since elements of the simulation environment are implemented as separate software modules, every element can be executed irrespective of other elements. Elements are executed by invoking Matlab scripts, that correspond to each element. This correspondence is shown in Table XIII.

An illustration of usage and operation of the simulation environment is shown in Figs. 52, 53, 54. Fig. 52 shows the usage of exposure generator, Fig. 53 shows the usage of exposure replayer, Fig. 54 shows the usage of statistical analyzer. The illustrations were captured directly from the Matlab work window. In the mentioned scripts, symbol ">>" presents Matlab command prompt. Textual lines following the command prompt are generated by the various scripts of the simulation environment.

A sample of the ATP script generated by the exposure generator is given in Appendix A. This sample is an example of how models of power network, instrument transformers and IEDs are integrated and used together. The ATP script in Appendix A describes a fault on the Sky-STP transmission line, where instrument transformers are connected at the Sky bus. This ATP script is inserted into the ATP script of the power network model (by the exposure generator) for simulation of power system events.

Table XIII. Correspondence between elements and scripts

Element	**Scripts**
Exposure generator	exposures.m
Exposure replayer	oc_test.m d_test.m
Statistical analyzer	oc_data.m d_data.m
Data formatter	oc_average.m d_average.m

```
>> init
INITIALIZATION
>> exposures
EXPOSURE GENERATOR
\results\ct_1\exposures\FAULT_Sky_Spr_AG___r0__l10_t1.mat modified
Elapsed time: 30.625 s
\results\ct_2\exposures\FAULT_Sky_Spr_AG___r0__l10_t1.mat modified
Elapsed time: 28.981 s
\results\ct_3\exposures\FAULT_Sky_Spr_AG___r0__l10_t1.mat modified
Elapsed time: 29.463 s
\results\ct_4\exposures\FAULT_Sky_Spr_AG___r0__l10_t1.mat modified
Elapsed time: 29.362 s
\results\ccvt_1\exposures\FAULT_Sky_Spr_AG___r0__l10_t1.mat modified
Elapsed time: 29.002 s
\results\ccvt_2\exposures\FAULT_Sky_Spr_AG___r0__l10_t1.mat modified
Elapsed time: 28.521 s
\results\ccvt_3\exposures\FAULT_Sky_Spr_AG___r0__l10_t1.mat modified
Elapsed time: 28.15 s
\results\ccvt_4\exposures\FAULT_Sky_Spr_AG___r0__l10_t1.mat modified
Elapsed time: 28.531 s
WARNING: node2 for ct changed
\results\ct_1\exposures\FAULT_Sky_Stp_AG___r0__l10_t1.mat modified
Elapsed time: 28.561 s
WARNING: node2 for ct changed
\results\ct_2\exposures\FAULT_Sky_Stp_AG___r0__l10_t1.mat modified
Elapsed time: 28.541 s
WARNING: node2 for ct changed
\results\ct_3\exposures\FAULT_Sky_Stp_AG___r0__l10_t1.mat modified
Elapsed time: 28.141 s
WARNING: node2 for ct changed
\results\ct_4\exposures\FAULT_Sky_Stp_AG___r0__l10_t1.mat modified
Elapsed time: 28.15 s
WARNING: node2 for ct changed
\results\ccvt_1\exposures\FAULT_Sky_Stp_AG___r0__l10_t1.mat modified
Elapsed time: 28.161 s
WARNING: node2 for ct changed
\results\ccvt_2\exposures\FAULT_Sky_Stp_AG___r0__l10_t1.mat modified
Elapsed time: 28.521 s
WARNING: node2 for ct changed
\results\ccvt_3\exposures\FAULT_Sky_Stp_AG___r0__l10_t1.mat modified
Elapsed time: 28.541 s
WARNING: node2 for ct changed
\results\ccvt_4\exposures\FAULT_Sky_Stp_AG___r0__l10_t1.mat modified
Elapsed time: 28.15 s
```

Fig. 52. Illustration of the exposure generator operation

```
>> oc_test
[0] Processing file ct_1:FAULT_Sky_Spr_AG___r0__l10_t1.mat...done
[1] Processing file ct_1:FAULT_Sky_Stp_AG___r0__l10_t1.mat...done
[2] Processing file ct_2:FAULT_Sky_Spr_AG___r0__l10_t1.mat...done
[3] Processing file ct_2:FAULT_Sky_Stp_AG___r0__l10_t1.mat...done
[4] Processing file ct_3:FAULT_Sky_Spr_AG___r0__l10_t1.mat...done
[5] Processing file ct_3:FAULT_Sky_Stp_AG___r0__l10_t1.mat...done
[6] Processing file ct_4:FAULT_Sky_Spr_AG___r0__l10_t1.mat...done
[7] Processing file ct_4:FAULT_Sky_Stp_AG___r0__l10_t1.mat...done
[8] Processing file ct_ref:FAULT_Sky_Spr_AG___r0__l10_t1.mat...done
[9] Processing file ct_ref:FAULT_Sky_Stp_AG___r0__l10_t1.mat...done
[10] Processing file ccvt_1:FAULT_Sky_Spr_AG___r0__l10_t1.mat...done
[11] Processing file ccvt_1:FAULT_Sky_Stp_AG___r0__l10_t1.mat...done
[12] Processing file ccvt_2:FAULT_Sky_Spr_AG___r0__l10_t1.mat...done
[13] Processing file ccvt_2:FAULT_Sky_Stp_AG___r0__l10_t1.mat...done
[14] Processing file ccvt_3:FAULT_Sky_Spr_AG___r0__l10_t1.mat...done
[15] Processing file ccvt_3:FAULT_Sky_Stp_AG___r0__l10_t1.mat...done
[16] Processing file ccvt_4:FAULT_Sky_Spr_AG___r0__l10_t1.mat...done
[17] Processing file ccvt_4:FAULT_Sky_Stp_AG___r0__l10_t1.mat...done
Elapsed time: 23.143 s
```

Fig. 53. Illustration of the exposure replayer operation

```
>> d_data
[1] Processing D file ct_1:D_D_Sky_Spr_AG___r0__l10_t1.mat...done
[2] Processing D file ct_1:D_D_Sky_Stp_AG___r0__l10_t1.mat...done
Created \results\ct_1\d_ag__\DDATA_ct_1.mat
[1] Processing D file ct_2:D_D_Sky_Spr_AG___r0__l10_t1.mat...done
[2] Processing D file ct_2:D_D_Sky_Stp_AG___r0__l10_t1.mat...done
Created \results\ct_2\d_ag__\DDATA_ct_2.mat
[1] Processing D file ct_3:D_D_Sky_Spr_AG___r0__l10_t1.mat...done
[2] Processing D file ct_3:D_D_Sky_Stp_AG___r0__l10_t1.mat...done
Created \results\ct_3\d_ag__\DDATA_ct_3.mat
[1] Processing D file ct_4:D_D_Sky_Spr_AG___r0__l10_t1.mat...done
[2] Processing D file ct_4:D_D_Sky_Stp_AG___r0__l10_t1.mat...done
Created \results\ct_4\d_ag__\DDATA_ct_4.mat
[1] Processing D file ct_ref:D_D_Sky_Spr_AG___r0__l10_t1.mat...done
[2] Processing D file ct_ref:D_D_Sky_Stp_AG___r0__l10_t1.mat...done
Created \results\ct_ref\d_ag__\DDATA_ct_ref.mat
[1] Processing D file ccvt_1:D_D_Sky_Spr_AG___r0__l10_t1.mat...done
[2] Processing D file ccvt_1:D_D_Sky_Stp_AG___r0__l10_t1.mat...done
Created \results\ccvt_1\d_ag__\DDATA_ccvt_1.mat
[1] Processing D file ccvt_2:D_D_Sky_Spr_AG___r0__l10_t1.mat...done
[2] Processing D file ccvt_2:D_D_Sky_Stp_AG___r0__l10_t1.mat...done
Created \results\ccvt_2\d_ag__\DDATA_ccvt_2.mat
[1] Processing D file ccvt_3:D_D_Sky_Spr_AG___r0__l10_t1.mat...done
[2] Processing D file ccvt_3:D_D_Sky_Stp_AG___r0__l10_t1.mat...done
Created \results\ccvt_3\d_ag__\DDATA_ccvt_3.mat
[1] Processing D file ccvt_4:D_D_Sky_Spr_AG___r0__l10_t1.mat...done
[2] Processing D file ccvt_4:D_D_Sky_Stp_AG___r0__l10_t1.mat...done
Created \results\ccvt_4\d_ag__\DDATA_ccvt_4.mat
Elapsed time: 1.623 s
```

Fig. 54. Illustration of the statistical analyzer operation

J. Integration of Different Models

Simulation environment can be used with different power network, instrument transformer and IED models. The recommendations for use of different models is as follows:

- Power network model is defined by ATP script, that contains description of the network. The location of the mentioned ATP script is defined in variable **power_network_model** (global variable) in script "init.m". Different power network models can be created as standard ATP scripts. ATP scripts should be stored within "models" directory of the root directory.

- Instrument transformers are defined by Matlab scripts "ct_model.m" and "vt_model.m". Different instrument transformer models can be created using the template stored in the mentioned Matlab scripts. Additional files (such as files "HYST.PCH", which define hysteresis curves) should be stored in "models" directory of the root directory.

- IED models are defined by Simulink models. Location of these models can be specified using Matlab and Simulink search path setting (see reference [33] for specific instructions). Names of IED Simulink models are specified in scripts "overcurrent.m" and "distance.m". Different IED models can be defined by specifying their names in the two mentioned script files. Different models must follow the communication channels (between simulation environment and Simulink) specified in Fig. 51. It is also important to store IED models response in the following variables:

  - **i_in**, **v_in** contain input current and voltage signals (from exposures, see Fig. 45)

– **i_abc**, **v_abc**, **I_abc**, **V_abc** receive output signals from the measuring element (see Chapter V)

– **trip** receives output from the decision making element (see Chapter V)

K. Conclusion

Simulation environment and its software implementation were described in this chapter. Simulation environment is a practical contribution of this thesis. It is implemented in form of software modules. One of the goals of the simulation environment is its expendability. This means that software was developed in such a way, that user can modify or add software modules, according to his/her research objectives. Special attention was paid to explanation of I/O data structure and flowchart of the environment. Three major elements of the environment are: 1) exposure generator, 2) exposure replayer and 3) statistical analyzer. Implementation of the elements was described and discussed first. Afterwards, user interface was explained. Together, major elements and user interface form a comprehensive software package.

Conclusion is that simulation environment can be used for extensive research in the area of instrument transformer evaluation. Simulation environment offers seamless interaction between several software packages, such as ATP, Matlab and Simulink. This interaction enables incorporation of wide variety of models of instrument transformers and IEDs. Possible applications of the simulation environment, beside evaluation of influence of instrument transformers, include evaluation of instrument transformer response, comparison of different instrument transformer designs, etc.

CHAPTER VII

EVALUATION METHODOLOGY APPLICATION AND RESULTS

A. Introduction

This chapter presents application of the evaluation methodology. Results are obtained by using simulation environment described in the previous chapter. As described in Chapter VI, final results present *average values* of performance indices. Average values were calculated according to the structure of the databases, as explained in Chapter VI.

B. Impact on the IED Model A

IED model A has outputs available at both measuring element (current and voltage) and decision making element (see section C of Chapter V). Therefore, influence of instrument transformers on both elements was evaluated. Evaluation criteria is listed and explained in Chapter IV. The results are presented in the following sections.

1. Interpretation of Performance Indices for the Measurement Element

In order to interpret the values of performance indices for the measurement element, it is necessary to define what values of the indices are indication of expected ("good") performance, and what values are indication of unexpected ("bad") performance. Generally, the lower the value, the better (more expected) the performance. However, since it is unrealistic to expect zero values, the following values can be used as indication of acceptable performance:

- Settling time ($t_{2\%}$) should be less than eight signal periods, i.e. 0.133 s
- Overshoot ($\Delta y_{\%}$) should be less than 10 %

- Absolute value of normalized error index ($|\Delta e_{\%}|$) should be less than 5 %
- Gain for DC component (FR_{DC}) should be less than 30 %
- Aggregated index (F) should be less than 0.01

The chosen values simply reflect the preferences of the author. Selection of the above mentioned values follows the practice defined in reference [16]. The values are also based around typical average of the performance indices of the referent instrument transformer.

2. Measurement Element Performance Indices

Values of performance indices for current measurement element of IED model A are shown in Tables XIV through XVI. Values for voltage measurement element are shown in Tables XVII through XIX.

Table XIV. Current measuring element, ABCG fault

Model	$t_{2\%}$	$\Delta y_{\%}$	$\Delta e_{\%}$	FR_{DC}	F
Referent	0.126	0.082	0.019	0.283	0.004
CT 1	0.126	0.079	0.070	0.175	0.005
CT 2	0.126	0.015	0.551	0.036	0.006
CT 3	0.126	0.100	0.054	0.215	0.005
CT 4	0.126	0.047	0.164	0.073	0.005

Table XV. Current measuring element, AG fault

Model	$t_{2\%}$	$\Delta y_{\%}$	$\Delta e_{\%}$	FR_{DC}	F
Referent	0.126	0.041	0.026	0.055	0.003
CT 1	0.126	0.044	0.100	0.038	0.003
CT 2	0.107	0.024	0.318	0.022	0.003
CT 3	0.126	0.045	0.052	0.041	0.003
CT 4	0.117	0.039	0.168	0.030	0.003

Table XVI. Current measuring element, BC fault

Model	$t_{2\%}$	$\Delta y_{\%}$	$\Delta e_{\%}$	FR_{DC}	F
Referent	0.126	0.056	0.052	0.193	0.004
CT 1	0.126	0.055	0.115	0.127	0.004
CT 2	0.126	0.010	0.452	0.020	0.005
CT 3	0.126	0.070	0.085	0.150	0.004
CT 4	0.126	0.044	0.184	0.059	0.004

Table XVII. Voltage measuring element, ABCG fault

Model	$t_{2\%}$	$\Delta y_{\%}$	$\Delta e_{\%}$	FR_{DC}	F
Referent	0.126	0.029	-0.004	0.022	0.003
CCVT 1	0.126	0.043	0.000	0.018	0.002
CCVT 2	0.126	0.140	-0.001	0.018	0.003
CCVT 3	0.126	0.048	0.000	0.018	0.002
CCVT 4	0.126	0.179	-0.006	0.019	0.003

Table XVIII. Voltage measuring element, AG fault

Model	$t_{2\%}$	$\Delta y_{\%}$	$\Delta e_{\%}$	FR_{DC}	F
Referent	0.065	0.009	-0.035	0.011	0.001
CCVT 1	0.065	0.011	-0.030	0.011	0.001
CCVT 2	0.065	0.025	-0.030	0.011	0.001
CCVT 3	0.065	0.010	-0.030	0.011	0.001
CCVT 4	0.065	0.029	-0.031	0.011	0.001

Table XIX. Voltage measuring element, BC fault

Model	$t_{2\%}$	$\Delta y_{\%}$	$\Delta e_{\%}$	FR_{DC}	F
Referent	0.065	0.017	-0.153	0.010	0.001
CCVT 1	0.065	0.013	-0.150	0.008	0.001
CCVT 2	0.065	0.026	-0.150	0.008	0.001
CCVT 3	0.065	0.016	-0.150	0.008	0.001
CCVT 4	0.065	0.031	-0.150	0.008	0.001

The following conclusions can be made, based on performance indices of the current measuring element:

- Influence of instrument transformer models on the settling time is relatively negligible (or small).
- Influence of instrument transformer models on overshoot varies significantly. Smallest overshoot is caused by current transformer model 2. Overshoot caused by this model is several times lower than the one caused by the referent instrument transformer. Significant decrease in overshoot indicates current transformer saturation, as discussed in Chapter IV. Current transformer model 4 shows slightly larger overshoot than model 2, while the rest of models caused overshoot levels close to what is found in the referent one.
- Influence on normalized error index also varies significantly. As in the case of overshoot, current transformer model 2 caused largest error, in the range from 30 % to 56 %. This error range is significant, and indicates possible misoperation by IED. Current transformer model 4 caused an increased error, at the level of 16 %, while the rest of the models did not cause the error to increase above 7 %.
- Influence on DC gain showed that current transformer model 2 suppresses DC component better than the rest of the models. Since it was already concluded that current transformer model 2 underwent saturation in significant number of test cases, it can be concluded that saturation actually enhances suppression of DC component. Current transformer model 4 also showed good DC suppression, compared to the rest of the models.
- Influence of instrument transformer models on aggregated frequency index is

negligible .

The following conclusions can be made, based on performance indices of voltage measuring element:

- CCVT models do not influence the settling time.
- CCVT models 2 and 4 caused significantly higher overshoot than for the referent one (overshoot is at least two times higher). The reason for this is the nature of the burden connected to model 2 and 4: inductive. Other models did cause slightly increased overshoot, than the referent model.
- The influence of instrument transformer models is relatively negligible (or small) on normalized error index. The same holds true for the influence on DC gain and aggregated frequency index.

3. Decision Making Element Performance Indices

Values of performance indices for decision making element of IED model A are shown in Tables XX through XXII. Note: mentioned performance indices for decision making element need a further clarification. Basis criteria is defined in Chapter IV. Meaning of indices in Tables XX through XXII is:

- N_1 is number of correct trip assertions for faults in forward direction of protection
- F_1 is number of incorrect trip restrains for faults in forward direction
- N_2 is number of correct trip restrains for faults in backward direction
- F_2 is number of incorrect trip assertions for faults in backward direction

- s_1 is defined as:

$$s_1 = \frac{N_1}{N_{forward}} \tag{7.1}$$

- s_2 is defined as:

$$s_2 = \frac{N_2}{N_{backward}} \tag{7.2}$$

where $N_{forward} = 48$ is number of faults simulated in forward zone of protection, and $N_{backward} = 16$ is number of faults simulated in backward zone. Ideal IED performance would produce $N_1 = 48$ and $N_2 = 16$. The rest of performance indices are listed and defined in Chapter IV.

The following conclusions can be made, based on the results:

- Current transformer model 2 caused the poorest performance of IED model. Detection of ABCG faults is impacted the most, while AG and BC faults are detected slightly better. The influence of current transformer model 2 is degrading IED model performance to unacceptable levels in the case of all three faults.

- Current transformer models, other than current transformer model 2, showed no influence on decision making element of IED model A. Current transformer model 4 did lower selectivity of IED model in backward zone slightly.

Table XX. Overcurrent decision element, ABCG fault

Model	N_1	F_1	N_2	F_2	s_1	s_2	t[s]
Referent	48	0	16	0	1	1	0.021
CT 1	48	0	16	0	1	1	0.025
CT 2	32	16	12	4	0.667	0.750	0.023
CT 3	48	0	16	0	1	1	0.022
CT 4	48	0	16	0	1	1	0.019
CCVT 1	48	0	16	0	1	1	0.021
CCVT 2	48	0	16	0	1	1	0.021
CCVT 3	48	0	16	0	1	1	0.021
CCVT 4	48	0	16	0	1	1	0.021

Table XXI. Overcurrent decision element, AG fault

Model	N_1	F_1	N_2	F_2	s_1	s_2	t[s]
Referent	48	0	16	0	1	1	0.009
CT 1	48	0	16	0	1	1	0.010
CT 2	43	5	9	7	0.896	0.563	0.012
CT 3	48	0	16	0	1	1	0.009
CT 4	48	0	13	3	1	0.813	0.012
CCVT 1	48	0	16	0	1	1	0.009
CCVT 2	48	0	16	0	1	1	0.009
CCVT 3	48	0	16	0	1	1	0.009
CCVT 4	48	0	16	0	1	1	0.009

Table XXII. Overcurrent decision element, BC fault

Model	N_1	F_1	N_2	F_2	s_1	s_2	t[s]
Referent	48	0	16	0	1	1	0.024
CT 1	48	0	16	0	1	1	0.028
CT 2	32	16	16	0	0.667	1	0.059
CT 3	48	0	16	0	1	1	0.025
CT 4	48	0	16	0	1	1	0.046
CCVT 1	48	0	16	0	1	1	0.024
CCVT 2	48	0	16	0	1	1	0.024
CCVT 3	48	0	16	0	1	1	0.024
CCVT 4	48	0	16	0	1	1	0.024

C. Impact on the IED Model B

IED model B has output available only for decision making elements. Values of performance indices for decision making element of IED model B are shown in Tables XXIII through XXV. Meaning of indices in Tables XX through XXII, based on criteria defined in Chapter IV, is:

- N_1 is number of correct trip assertions for faults in primary zone of protection
- F_1 is number of trip assertions with incorrect time-delay, for faults in primary zone of protection (faults detected as belonging to backup zone)
- N_2 is number of correct trip assertions for faults in backup zone of protection
- F_2 is number of trip assertions with incorrect time-delay, for faults in backup zone of protection (faults detected as belonging to primary zone)
- s_1 is defined as:

$$s_1 = \frac{N_1}{N_{primary}} \tag{7.3}$$

- s_2 is defined as:

$$s_2 = \frac{N_2}{N_{backup}} \tag{7.4}$$

where $N_{primary} = 32$ is number of faults simulated in primary zone of protection, and $N_{backup} = 32$ is number of faults simulated in backup zone. Ideal IED performance would produce $N_1 = 32$ and $N_2 = 32$. Indices t_1 and t_2 are average tripping times for faults in primary and backup zones, respectively (average tripping time is calculated only for correct trip assertions). In cases where t_2 could not be calculated because of IED model misoperation (e.g. none of the faults in zone 2 were recognized), an asterisk (*) was placed in the Table entries (corresponding to the mentioned cases).

The following conclusions can be made, based on the results:

Table XXIII. Distance decision element, ABCG fault

Model	N_1	F_1	N_2	F_2	s_1	s_2	t_1[s]	t_2[s]
Referent	32	0	28	4	1	0.875	0.017	0.043
CT 1	32	0	32	0	1	1	0.018	0.043
CT 2	32	0	0	32	1	0	0.016	*
CT 3	32	0	32	0	1	1	0.018	0.043
CT 4	32	0	0	32	1	0	0.015	*
CCVT 1	32	0	28	4	1	0.875	0.017	0.043
CCVT 2	32	0	32	0	1	1	0.017	0.043
CCVT 3	32	0	28	4	1	0.875	0.017	0.043
CCVT 4	32	0	28	4	1	0.875	0.017	0.043

Table XXIV. Distance decision element, AG fault

Model	N_1	F_1	N_2	F_2	s_1	s_2	t_1[s]	t_2[s]
Referent	32	0	32	0	1	1	0.035	0.043
CT 1	24	8	32	0	0.750	1	0.039	0.043
CT 2	17	15	32	0	0.531	1	0.035	0.043
CT 3	32	0	32	0	1	1	0.036	0.043
CT 4	20	12	32	0	0.625	1	0.037	0.043
CCVT 1	32	0	32	0	1	1	0.034	0.043
CCVT 2	32	0	32	0	1	1	0.035	0.043
CCVT 3	32	0	32	0	1	1	0.034	0.043
CCVT 4	32	0	32	0	1	1	0.034	0.043

Table XXV. Distance decision element, BC fault

Model	N_1	F_1	N_2	F_2	s_1	s_2	t_1[s]	t_2[s]
Referent	32	0	28	4	1	0.875	0.017	0.043
CT 1	32	0	32	0	1	1	0.018	0.043
CT 2	32	0	8	24	1	0.250	0.017	0.040
CT 3	32	0	32	0	1	1	0.018	0.043
CT 4	32	0	14	18	1	0.438	0.017	0.040
CCVT 1	32	0	28	4	1	0.875	0.017	0.043
CCVT 2	32	0	32	0	1	1	0.017	0.043
CCVT 3	32	0	28	4	1	0.875	0.017	0.043
CCVT 4	32	0	28	4	1	0.875	0.017	0.043

- From performance of IED model B connected to referent instrument transformers, it can be seen that IED model shows small overreach for ABCG and BC fault types (selectivity in zone 2 is 87.5 %). However, IED model B showed no overreach effects when connected to current transformer models 1 and 3, and CCVT model 2. It can be concluded that mentioned instrument transformer models have positive influence on IED model B. However, this positive influence of mentioned instrument transformer models does not remove IED model's inherent internal problem of overreach. If the IED model B had not been tested using the referent model, the inherent overreach would not be discovered. Mentioned instrument transformer models masked (hid) the overreach.

- Current transformer models 2 and 4 caused IED model to overreach complete zone 2 for ABCG fault type. The reason for this is larger error in measurement, cause by mentioned current transformer models.

D. Conclusion

This chapter presented results from application of the evaluation methodology. Results were obtained using the simulation environment. Methodology is described in Chapter V, while simulation environment is presented in Chapter VI. Results confirm existing observation about influence of instrument transformers of IED performance. Results also point-out to some new aspects of this influence, which have not been presented in literature so far.

Observations that can be made, based on results from the application of methodology, are:

- Influence of various instrument transformer models differs significantly. In general, CCVT models (which include models of voltage transformers) have significantly smaller impact on IED model performance. This indicates that in practice, voltage transforming devices (voltage transformers and CCVTs) are expected to cause IED misoperations in extremely small number of cases. It can be hard to even detect these influences using field-recorded data. Simulation environment is, therefore, a useful tool in analyzing situations when corrupting influence of CCVTs is suspected.

- Influence of current transformer models varies significantly from one model to another. Main cause of differences are model parameters. In general, burden magnitude and VI characteristic of electromagnetic core are two major sources of corruptive instrument transformer influence. This is confirmed by the results.

- Saturation, phenomena associated with current transformers, actually enhances certain aspects of current transformer response. Results have shown that, for example, measuring algorithm suppresses the DC offset better for input signals supplied from a saturated current transformer. Simulation environment is a useful tool in further researching of this effect.

- Distortions in IED input signals may lead to a better IED performance, compared to performance of IED supplied with undistorted input signals. Even though this may seem as a desired influence of instrument transformers, it is not. Bad performance (such as overreaching, which was demonstrated in the results) can be masked, i.e. not detected, when connected to current transformers that cause signal distortions. This is an important observation for transient testing of IEDs. Simulation environment can be used as supplement to existing testing tools to investigate transient response of the protective relays in more detail, regarding the mentioned hiding (masking).

Conclusion is that results, delivered by simulation environment, are comprehensive and meaningful. It was presented how various instrument transformer aspects influence elements of IEDs, and how this influence shapes the performance of IEDs. Therefore, simulation environment was shown, through application, to be a useful and novel tool for analysis of the influence of instrument transformers on protective IED performance.

CHAPTER VIII

CONCLUSION

A. Summary

Instrument transformers (IT) are crucial components of power protection system. Their objective is to supply scaled-down replicas of power network current and voltage signals. Depending on accuracy of these replicas, faulty conditions are recognized and properly and timely dealt with by protection system. This, in turn, affects the operation of power system.

Conventional instrument transformer are based on electromagnetic coupling between power network on the primary side, and protective devices on the secondary side. Side-effect of this coupling are signal distortions. Protective devices and other IEDs are sensitive to these distortions. This sensitivity can lead to misoperation, which consequently, may lead to disruption of power system operation.

A way of overcoming this problem is introducing novel, optical instrument transformers, called transducers. The improvement, made possible by the new current and voltage sensing technology, is enabling distortion-free replicas of signals from the primary side of transducers. However, these improvements are still barely tested through field application experiences.

There is still an uncertainty about whether the new technology is superior to the conventional one. This uncertainty is summarized by questions:

1. What is the difference in performance between the conventional instrument transformers and novel, optical transducers ?

2. How can this difference be practically measured or evaluated ?

Existing approaches to solving the problem, available in the literature, do not offer systematic and comprehensive answers to these questions. On the other hand, the answer is necessary to asses benefits of the new technology. This thesis proposes a new methodology for evaluation of influence of instrument transformers on IED performance. Existing approaches focus mostly on evaluation of either instrument transformer response, or IED performance. Difference between methodology presented in this thesis and existing ones, is that the proposed methodology is combining mentioned approaches into unique a procedure. This procedure can lead to answers to the mentioned questions.

While developing and applying the methodology, several steps were taken. Steps are described in various chapters of this thesis. First, instrument transformer performance characteristics were analyzed in Chapter II. It was shown that instrument transformer performance characteristics are the root of distortions. Various instrument transformer designs were discussed. Three performance characteristics were identified as having the major impact on generation of distortions: accuracy, frequency bandwidth and transient response. Impact of mentioned characteristics on distortions was described. It was concluded that distortions can be significant.

Sensitivity of protective devices to distortions was addressed in Chapter III. It was shown that protective devices do not show degradation in performance when exposed to signal distorted up to a certain threshold level. However, distortion levels above the threshold cause IEDs to miss-operate. Miss-operation includes unacceptably high increase of operationing time and/or unacceptably low selectivity. It was concluded that distortions caused by conventional instrument transformers can lead to IED misoperation.

Criteria and new methodology for evaluation of the influence of instrument transformers was presented in Chapter IV. Criteria was defined for measuring and decision making elements of protective IEDs. Some problems, when calculating numerical values for the criteria, and how to overcome the problems were also addressed. The new methodology covered important aspects of evaluation: 1) why is evaluation important, 2) what are the means for quantifying the influence (finding numerical values), 3) what is the best procedure for finding the quantitative values of the influence, 4) what is the meaning of the quantitative values. It was concluded that new methodology presents systematic and comprehensive approach to the problem solution.

Simulation approach to evaluation was described in Chapter V. Main aspects of simulation, models and scenarios, were discussed. First, simulation procedure was discussed. Power network, instrument transformer and IED models were presented, along with reasoning for the choice. Simulation scenarios were presented next. It was concluded that, by proper choice of models and proper scenario definitions, meaningful results can be obtained through simulation.

Simulation environment, which presents software implementation of the methodology, was presented in Chapter VI. The environment enables seamless interaction between several software packages. The environment is implemented in form of software modules. Three main modules, exposure generator, exposure replayer and statistical analyzer, were described in detail. Particular importance was placed on description of I/O data structure and flowchart. These aspects are important for the users who wish to modify or expand the environment. It was concluded that environment presents a useful tool for application of the methodology.

Application of evaluation methodology was presented in Chapter VII. Results obtained through simulation were presented. Results both confirmed existing observations and offered some new insights, considering influence of instrument transformers on protective IEDs. New insights include: certain distortions (such as the one caused by saturation) can be detected by analyzing numerical values of performance indices, instrument transformers can mask (hide) bad IED performance. It was concluded that simulation environment can be used for obtaining meaningful and comprehensive results.

Thesis contributions are both theoretical and practical. Both contributions are summarized in the next section.

B. Contribution

At present, there is no comprehensive and systematic methodology for evaluation of the influence of instrument transformers on protective IEDs. The main contribution of this thesis is a new methodology for evaluation.

Theoretical contributions of the thesis are:

- Connection between instrument transformer characteristics, signal distortions and IED sensitivity was established (Chapters II and III). It was shown that instrument transformer characteristic have direct impact on IED performance, and therefore may affect power system operation.

- Criteria and methodology for evaluation of the influence of instrument transformers was defined (Chapter IV). Criteria was defined in form of numerical performance indices. Methodology was defined through steps for the evaluation procedure.

Practical contributions of the thesis are:

- Modelling and simulation approach to evaluation of influence of instrument transformers was established (Chapter V). It was shown how to choose models in order to achieve meaningful results through simulation.

- Simulation environment was developed (Chapter VI). Environment is in the form of software modules. Environment was shown to be a useful tool in analyzing influence of instrument transformers. Other benefits of the environment include its modifiability and expendability.

- Methodology was applied through simulations, using developed simulation environment (Chapter VII). It was shown that this approach can successfully provide information about influence of instrument transformer characteristics on IED performance. The results can be used for further research.

REFERENCES

[1] P. M. Anderson, *Power System Protection*, New York, NY: McGraw-Hill, 1999, p. 23-34.

[2] J. L. Blackburn, *Protective Relaying: Principles and Applications*, New York, NY: Marcel Dekker, 1998, p. 26-28, 129-141, 151-157.

[3] C. Christos, A. Wright, *Electrical Power System Protection*, Boston, MA: Kluwer Academic Publishers, 1999, p. 39-103.

[4] Power Systems Communication Committee, Working Group Fiber Optics Sensors of the Fiber Optics Subcommittee, "Optical current transducers for power systems: A review," *IEEE Transactions on Power Delivery*, vol. 9, no. 4, pp. 1778-1788, October 1994.

[5] Power Systems Relaying Committee, Working Group of the Relay Input Sources Subcommittee, "Transient response of current transformers," *IEEE Transactions on Power Apparatus and Systems*, vol. 96, no. 6, pp. 1809-1814, November 1977.

[6] Power Systems Relaying Committee, Working Group of the Relay Input Sources Subcommittee, "Transient response of coupling capacitor voltage transformers," *IEEE Transactions on Power Apparatus and Systems*, vol. 100, no. 12, pp. 4811-4814, December 1981.

[7] M.I. Samesima, J.C. de Oliveira, E.M. Dias, "Frequency response analysis and modeling of measurement transformers under distorted current and voltage supply," *IEEE Transactions on Power Delivery*, vol. 6, no. 4, pp. 1762-1768, October 1991.

[8] M. Kezunovic, C. Fromen, F. Phillips, Lj. Kojovic, A. Abur, D. Sevcik, "Experimental evaluation of EMTP based current transformer models for protective relay transient study," *IEEE Transactions on Power Delivery*, vol. 9, no. 1, pp. 405-413, January 1994.

[9] D. Tziouvaras, P. McLaren, C. Alexander, D. Dawson, J. Esztergalyos, C. Fromen, M. Glinkowski, I. Hasenwinkle, M. Kezunovic, L. Kojovic, B. Kotheimer, R. Ruffel, J. Nordstrom, S. Zochol, "Mathematical models for current, voltage and coupling capacitor voltage transformers," *IEEE Transactions on Power Delivery*, vol. 15, no. 1, pp. 62-72, January 2000

[10] M. Kezunovic, A. Abur, Lj. Kojovic, V. Skendzic, H. Singh, "DYNA-TEST simulator for relay testing, Part II: Performance evaluation," *IEEE Transactions on Power Delivery*, vol. 7, no. 3, pp. 1097-1103, July 1992.

[11] J.R. Lucas, P.G. McLaren, W.W.L. Keerthipala, R.P. Jayasinghe, "Improved simulation models for current and voltage transformers in relay studies," *IEEE Transactions on Power Delivery*, vol. 7, no. 1, pp. 152-159, January 1992.

[12] P.G. McLaren, R.P. Jayasinghe, "Simulation of CTs operating in parallel in a differential current protection scheme," in *Proceedings of IEEE Communications, Power and Computing Conference*, vol. 1, no. 1, Winnipeg, MB, Canada, May 1997, pp. 126-131.

[13] M. Kezunovic, J.T. Cain, B. Perunicic, S. Kreso, "Digital protective relaying algorithm sensitivity study and evaluation," *IEEE Transactions on Power Delivery*, vol. 3, no. 3, pp. 912-922, July 1988.

[14] E. A. Udren, J. A. Zipp, "Proposed statistical performance measures for microprocessor-based transmission-line protective relays, Part I: Explanation of

the statistics," *IEEE Transactions on Power Delivery*, vol. 12, no. 1, pp. 134-143, January 1997.

[15] E. A. Udren, J. A. Zipp, "Proposed statistical performance measures for microprocessor-based transmission-line protective relays, Part II: Collection and uses of data," *IEEE Transactions on Power Delivery*, vol. 12, no. 1, pp. 144-156, January 1997.

[16] M. Kezunovic, B. Kasztenny, "Design optimization and performance evaluation of the relay algorithms, relays and protective systems using advanced testing tools," *IEEE Transactions on Power Delivery*, vol. 15, no. 4, pp. 1129-1135, October 2000.

[17] M.S. Sachdev, T.S. Sidhu, P.G. McLaren, "Issues and opportunities for testing numerical relays," in *Proceedings of IEEE Power Engineering Society Summer Meeting*, vol. 2, no. 1, New York, NY, May 1997, pp. 1185-1190.

[18] M. Kezunovic, Q. Chen, "A novel approach for interactive protection system simulation," *IEEE Transactions on Power Delivery*, vol. 12, no. 2, pp. 668-674, April 1997.

[19] M. Kezunovic, Y.Q. Xia, Y. Guo, C.W. Fromen, D.R. Sevcik, "Distance relay application testing using a digital simulator," *IEEE Transactions on Power Delivery*, vol. 12, no. 1, pp. 72-82, January 1997.

[20] M. Kezunovic, Y.Q. Xia, Y. Guo, C.W. Fromen, D.R. Sevcik, "An advanced method for testing of distance relay operating characteristic," *IEEE Transactions on Power Delivery*, vol. 11, no. 1, pp. 149-157, January 1996.

[21] M. Kezunovic, A. Abur, Lj. Kojovic, V. Skendzic, H. Singh, "DYNA-TEST

simulator for relay testing, Part I: Design characteristics," *IEEE Transactions on Power Delivery*, vol. 6, no. 4, pp. 1423-1429, October 1991.

[22] IEEE Standard C57.13-1993, *Requirements for Instrument Transformers*, IEEE, New York, NY, June 1993, pp. 1-73.

[23] CanAm EMTP User Group, *Alternative Transient Program (ATP) Rule Book*, Portland, OR, January 1992.

[24] Lj. Kojovic, M. Kezunovic, S.L. Nilsson, "Computer simulation of a ferroresonance suppression circuit for digital modeling of coupling capacitor voltage transformers," in *Proceedings of ISMM Conference on Computer Applications in Design, Simulation and Analysis*, vol. 1, no. 1, Orlando, FL, March 1992, pp. 20-24.

[25] R. C. Dugan, M. F. McGranaghan, H. W. Beaty, *Electrical Power Systems Quality*, New York, NY: McGraw-Hill, 1996, p. 1-38.

[26] Lj. A. Kojovic, "Impact of current transformer saturation on overcurrent protection operation," in *Proceedings of IEEE Power Engineering Society Summer Meeting*, vol. 3, no. 1, New York, NY, July 2002, pp. 1078-1083.

[27] M.A. Hughes, "Distance relay performance as affected by capacitor voltage transformers," *Proceedings of IEE*, vol. 121, no. 12, pp. 1557-1566, December 1974.

[28] W.D. Humpage, K.P. Wong, "Influence of capacitor-voltage-transfomers on the dynamic response of distance protection," *Electrical Engineering Transactions*, vol. 14, no. 2, pp. 59-63, June 1978.

[29] M. Kezunovic, A. Abur, G. Huang, "MERIT 2000 - A new concept in power engineering education," in *Proceedings of Energy Management and Power Delivery*

Conference, vol. 1, no. 1, Singapore, March 1998, pp. 54-59.

[30] H.O. Pascual, J.A. Rapallini, “Behaviour of Fourier, cosine and sine filtering algorithms for distance protection, under severe saturation of the current magnetic transformer,” in *Proceedings of IEEE Power Tech Conference*, vol. 4, no. 1, Porto, Portugal, September 2001, pp. 6-12.

[31] D. Ristanovic, S. Vasilic, M. Kezunovic, “Design and implementation of scenarios for evaluating and testing distance relays,” in *Proceedings of* 33^{rd} *North American Power Symposium*, vol. 1, no. 1, College Station, TX, October 2001, pp. 470-475.

[32] IEEE Standard C37.112-1996, *Inverse-Time Characteristic Equations for Overcurrent Relays*, IEEE, New York, NY, January, 1996, pp. 1-13.

[33] The MathWorks, Inc., *Using MATLAB*, Natick, MA, January 1999.

[34] The MathWorks, Inc., *Using Simulink*, Natick, MA, June 1990.

[35] The MathWorks, Inc., *Power System Blockset Users Guide*, Natick, MA, January 1999.

APPENDIX A

```
C ** FAULT DATA START **
/BRANCH
C ** CT MODEL CONNECTION DATA START **
-1SKY3A SKY1A            .435942.00994.3725150.69 0 0                       0
-2SKY3B SKY1B            .06143 .56647.6245150.69 0 0                       0
-3SKY3C SKY1C                                                               0
C ** CT MODEL START **
/BRANCH
  CTS1A CTSA               8.33  .175                                       0
/BRANCH
  CTS1B CTSB               8.33  .175                                       0
/BRANCH
  CTS1C CTSC               8.33  .175                                       0
/BRANCH
96      CTS1A               0.0   0.0                                       0
$INCLUDE, C:\ATP37\atp2\models\HYST_2.pch
96      CTS1B               0.0   0.0                                       0
$INCLUDE, C:\ATP37\atp2\models\HYST_2.pch
96      CTS1C               0.0   0.0                                       0
$INCLUDE, C:\ATP37\atp2\models\HYST_2.pch
/SOURCE
14CTS1A       1E-10      60.                                  -1.       10.
18             180.SKY3A CTPA
14CTS1B       1E-10      60.                                  -1.       10.
18             180.SKY3B CTPB
14CTS1C       1E-10      60.                                  -1.       10.
18             180.SKY3C CTPC
/SWITCH
        CTSA                                          MEASURING             1
        CTSB                                          MEASURING             1
        CTSC                                          MEASURING             1
  SKYA  CTPA                                          MEASURING             1
  SKYB  CTPB                                          MEASURING             1
  SKYC  CTPC                                          MEASURING             1
C ** CT MODEL END **
C == CCVT MODEL START ==
/BRANCH
  N2A   N3A                228.                                             0
  N1A   SKYA                         .82938                                 0
        N1A                          32.497                                 0
  N1A   N2A                    21997.                                       0
  N1A   N3A                          .03770                                 0
        N3A                          5.7E-8                                 0
```

```
  TRANSFORMER                         TA0001  5.E5                             0
           9999
 1N3A                  400. 1131. 8.586
 2VTA                    .2  .377  .112
  N5A   VTA                       3600.                                        0
  N5A   VTA                263.89                                              0
        N5A            37.5                                                    0
        VTA            100.                                                    0
  N2B   N3B            228.                                                    0
  N1B   SKYB                     .82938                                        0
        N1B                      32.497                                        0
  N1B   N2B                21997.                                              0
  N1B   N3B                      .03770                                        0
        N3B                      5.7E-8                                        0
  TRANSFORMER                         TB0001  5.E5                             0
           9999
 1N3B                  400. 1131. 8.586
 2VTB                    .2  .377  .112
  N5B   VTB                       3600.                                        0
  N5B   VTB                263.89                                              0
        N5B            37.5                                                    0
        VTB            100.                                                    0
  N2C   N3C            228.                                                    0
  N1C   SKYC                     .82938                                        0
        N1C                      32.497                                        0
  N1C   N2C                21997.                                              0
  N1C   N3C                      .03770                                        0
        N3C                      5.7E-8                                        0
  TRANSFORMER                         TC0001  5.E5                             0
           9999
 1N3C                  400. 1131. 8.586
 2VTC                    .2  .377  .112
  N5C   VTC                       3600.                                        0
  N5C   VTC                263.89                                              0
        N5C            37.5                                                    0
        VTC            100.                                                    0
/OUTPUT
  SKYA  SKYB  SKYC  VTA   VTB   VTC
C == CCVT MODEL END ==
/BRANCH
C ** CT MODEL CONNECTION DATA END **
-1SKY1A STPA          .435942.00994.372516.744 0 0                            0
-2SKY1B STPB          .06143 .56647.624516.744 0 0                            0
-3SKY1C STPC                                                                  0
/SWITCH
  SKY1A SKY1B    .064583       10.                                             0
/BRANCH
/SWITCH
  SKY1B SKY1C    .064583       10.                                             0
/BRANCH
/SWITCH
```

```
  SKY1A SKY2A    .064583       10.                                                0
/BRANCH
/BRANCH
        SKY2A                 5.                                                  0
C ** FAULT DATA END **
```

VITA

Bogdan Naodovic was born in 1977 in Novi Sad, Yugoslavia. He received his Bachelor of Science degree in electrical engineering (Diploma of Engineering) from the Faculty of Technical Sciences, University of Novi Sad, Yugoslavia, on December 29, 2001. In undergraduate studies, he majored in telecommunications.

Bogdan Naodovic entered graduate school at Texas A&M University in the Summer of 2002. His emphasis in graduate school was in the area of power systems and instrument transformers. During his graduate studies, he worked on various research assignments as a research assistant. He was also Power System Control and Protection Lab manager.

Author's address:

Texas A&M University

Department of Electrical Engineering

College Station, Texas 77843-3128